applied sciences

MDPI

Article

Use of a Yeast Protein-Based Intumescent Fire Retardant Bioadditive as Thermal and Mechanical Reinforcement for a PVAc Adhesive for Wood Products

Marcela Vidal-Vega [1,2,3,*], Mario Núñez-Decap [1,2], Diógenes Hernández-Espinoza [4,5] and Arturo Fernández-Pérez [6]

[1] Departamento de Ingeniería Civil y Ambiental, Facultad de Ingeniería, Universidad del Bío-Bío, Avenida Collao 1202, Concepción 4051381, Chile; mnunez@ubiobio.cl
[2] Centro Nacional de Excelencia Para la Industria de la Madera (ANID BASAL FB210015 CENAMAD), Pontificia Universidad Católica de Chile, Vicuña Mackenna 4860, Santiago 7820436, Chile
[3] Programa de Doctorado en Ingeniería, Facultad de Ingeniería, Universidad del Bío-Bío, Avenida Collao 1202, Concepción 4051381, Chile
[4] Department of Industrial Technologies, Faculty of Engineering, University of Talca, P.O. Box 747, Talca 3460000, Chile; dhernandez@utalca.cl
[5] Environmental Laboratory of Gases and Biofuels (LAGBIO), University of Talca, P.O. Box 747, Talca 3460000, Chile
[6] Departamento de Física, Facultad de Ciencias, Universidad del Bío-Bío, Avenida Collao 1202, Concepción 4051381, Chile; arturofe@ubiobio.cl
* Correspondence: mvidalve@ubiobio.cl; Tel.: +56-41-311-1799

Abstract: In this study, an intumescent fire retardant (IFR) bioadditive was designed based on a commercial *Saccharomyces cerevisiae* yeast protein matrix. Lignosulfonate was used as a cohesive reinforcement of its polymeric structure, along with magnesium hydroxide $Mg(OH)_2$, as agents that enhance the binder-intumescent properties, with the aim of improving the thermal stability and fire resistance of the commercial PVAc adhesive. Firstly, two formulations of the bioadditive were elaborated and characterized for their physicochemical and electrical properties, dynamic mechanical analysis (DMA), adherence properties (shear strength), and fire resistance, to modify the PVAc adhesive. Thus, it was found that the IFR bioadditive formulation with a higher percentage of $Mg(OH)_2$ was more thermally stable than the other one, although both of them were able to enhance the binder-intumescent properties of the commercial adhesive PVAc. Then, ten adhesive blends of PVAc modified with these two different bioadditives were added in different proportions, and were elaborated and characterized for their physicochemical and electrical properties, mechanical properties including a shear test (dry, elevated temperature, and three-cycle conditions) and delamination. Based on these results, five adhesive blends were selected, and we performed the following tests: adhesive penetration, fire resistance, volatile organic compounds (VOCs), and morphological and elemental analysis by scanning electron microscope (SEM/EDS). From the modified PVAc adhesive blends, two samples were selected, which were able to improve the high temperature and fire performance of a PVAc adhesive.

Keywords: protein; bioadditive; thermal reinforcement; intumescent fire-retardant (IFR); polyvinyl acetate (PVAc); wood products

Academic Editor: Roger Narayan

Received: 21 January 2025
Revised: 7 February 2025
Accepted: 10 February 2025
Published: 15 February 2025

Citation: Vidal-Vega, M.; Núñez-Decap, M.; Hernández-Espinoza, D.; Fernández-Pérez, A. Use of a Yeast Protein-Based Intumescent Fire Retardant Bioadditive as Thermal and Mechanical Reinforcement for a PVAc Adhesive for Wood Products. *Appl. Sci.* **2025**, *15*, 2051. https://doi.org/10.3390/app15042051

1. Introduction

Within the world of adhesives for wood, Polyvinyl Acetate (PVAc) adhesive is a water-based adhesive, which is considered more environmentally acceptable compared

to solvent-based adhesives. PVAc is most often used as an adhesive for porous materials such as wood and paper, but it is also a good adhesive for plastics, metal foil, leather, cloth, and as a general building adhesive. The main advantages of PVAc are its easy and wide application, elasticity, resistance to aging, low cost and availability, resistance to bacterial and fungicidal attack, and non-toxicity. Nevertheless, this adhesive also has some disadvantages related to its thermal and mechanical properties. PVAc has a thermoplastic nature and a linear amorphous structure, which makes it poorly resistant to temperature and relative humidity changes, affecting the adhesive bond quality. Also, due to its poor thermal stability, with a heat presence, this adhesive can yield because of a continuous load effect over time. To overcome these advantages, some studies evaluate the modification of PVAc, by adding different nanoparticles or additives, for example: nano clay (NC), cellulose nanofibrils (CNFs), silica (SiO_2), titanium dioxide (TiO_2) nanoparticles, and multi wall carbon nanotubes (MWCNTs) [1–6].

Unfortunately, unmodified polymers do not have ideal flame-retardant properties, however, flame-retardant polymer materials can be developed. This mechanism is intended to decrease the material's flammability and slow the flame's spread. When the flame is removed, it will quickly self-extinguish, halting the burning process. Flame retardant polymer materials can be classified into halogen, inorganic, organic, intumescent, and nano-filler flame retardants according to the type of fillers [7].

Halogenated fire retardants work by continuously releasing free radicals, interrupting the emission of gases. During the combustion of the substrate, high-energy OH and H radicals are generated, which react with the free radicals of the halogenated compounds, thus stopping the spread of fire [7,8]. Halogenated fire retardants have been in use for more than 40 years due to their good flame retardant performance [9]; however, there is great concern in the scientific and industrial environment, because their use generates negative impacts on the health of human beings and the environment [10,11]. Therefore, the challenge at the scientific and industrial level is related to the development of fire retardant products, free of halogen compounds, for the protection of a wide variety of materials, with high flame-retardant efficiency and economic convenience [12]. Intumescent fire-retardant systems (IFR) are among the existing efficient and very low-toxicity fire-retardant solutions. Fire retardant products, of an intumescent nature, with flame retardant applications, are composed of three fundamental elements:

(a) Coking agent. These are generally polyatomic alcohols or polyols (containing organic hydroxyl), i.e., compounds with a high carbon content.
(b) Catalysts (acid components). Here, inorganic acids or substances that release acid at a temperature between 100 and 250 °C are possible.
(c) Foaming agents. Mainly organic amines or amides, although some inorganic salts can release significant amounts of non-combustible gases after thermal decomposition (carbonates of alkali metals and ammonium salts, among others) [13]. In general, the most common synthetic fire-retardant intumescent systems (out of the commercial types), present three fundamental elements: carbon, nitrogen, and phosphorus. These decompose in the presence of heat into: a carbon part, which serves as a thermal insulator; a gaseous part, which with these gases dilutes the combustible gases in the combustion process; and, finally, an acidic part (phosphoric acid), which catalyzes or retards the advance of fire.

On the other hand, due to their intrinsic fire-retardant properties, proteins have opened an interesting opportunity for developing fire-retardant products [14]. Proteins, which have mainly been used for the development of bioadhesives for wood, have great potential because they require lower setting temperatures than those generally used in the industry [15,16]. For the manufacture of protein-based adhesives, proteins have been

extracted from yeast [17–22], wheat (gluten) [23,24], soybean meal, and cottonseed [25–28], among others. Following the general characteristics of proteins, several studies have revealed that their amino acid composition allows them to begin their decomposition at temperatures close to 100 °C, where amino acids rich in nitrogen and oligopeptides composed of carboxylic acid, catalyze the combustion process of the substrate, causing higher carbon volumes at temperatures exceeding 750 °C [9,29]. In the first stage of combustion, the presence of carbon and nitrogen-based elements acts. Finally, the element in charge of generating thermal insulating carbon, which is generally phosphorus-based, prevents heat transfer to the rest of the substrate [30].

In the past few years, developments of different protein-based flame retardant systems have been reported. In this regard, Petkovska et al., 2024 [31], developed an intumescent flame retardant coating based on egg white protein (EWP) and a solution of magnesium lignosulfonate (LS) plus diammonium phosphate (DAP) for cotton, defined as EWP/(LS-DAP). This study validates the potential of a product based on egg white proteins as an intumescent fire-retardant system capable of protecting a substrate such as cotton against the onslaught of fire. Dong et al., 2023 [32], synthesized a fire retardant for the polymer polylactic acid (PLA) based on soy protein modified with dimethyl phosphite (SPDP), which also contained phosphorus and nitrogen (P-N). This study established that SPDP is highly effective and could be an excellent replacement alternative to fossil-based flame retardants for improving the thermal performance of PLA. Xu et al., 2022 [33], synthesized a phosphorus–nitrogen bifunctional casein-based flame retardant (CADP), to be applied on pretreated cotton (D-cellulose) fabrics. The bio-based CADP was found to be highly effective as a fire retardant, and it could serve as a replacement for other conventional flame retardants for cotton fabrics. Chen et al., 2021 [34], developed a flame retardant (FR) based on arginine (protein amino acid) plus the incorporation of phosphorus and nitrogen. The FR was designed for application to Lyocell tissues. TGA and Raman analyses showed that FR-treated lyocell fibers exhibited high thermal stability and higher carbon volumes than untreated samples, indicating a significant improvement in the fire resistance of FR-modified lyocell. Vishwakarma et al., 2021 [35], developed a flame retardant based on egg white (W) protein with hypophosphorous acid (HA), applied in layers on cotton fibers. The W+HA-treated fabric exhibited high carbon formation with no afterglow effect. In addition, it showed excellent FR performance. Uddin et al., 2020 [36], developed a FR composite using a suspension of casein and $Mg(OH)_2$ to form a self-adhesive coating. Both casein and $Mg(OH)_2$ generated a synergistic state in the coating, significantly improving the fire resistance of the treated wood samples. Albite-Ortega et al., 2019 [37], used keratin fibers (KF), from bird feathers and deoxyribose nucleic acid (DNA), to be incorporated in mixtures of low-density polyethylene and ethylene vinyl acetate (PE/EVA). The DNA behaved as an intumescent agent and the keratin helped the formation of carbon in the combustion process, reducing the concentration of magnesium hydroxide from 55 to 20%, with improved mechanical properties.

As previously mentioned, proteins can also be found in yeasts, such as *Saccharomyces cerevisiae*, which is composed mainly of amino acids rich in nitrogen, phosphorus, and sulfur, as well as DNA and mineral salts (with flame retardant properties) [38]. The high concentrations of the proteins found in *Saccharomyces cerevisiae* yeasts make them very attractive for the development of IFR products, as their adhesive thermal stabilizing and fire resistance properties ensure affinity with water-soluble adhesive products such as PVAc adhesive.

On the other hand, magnesium hydroxide $Mg(OH)_2$, a compound identified as an inorganic salt, performs the function of fire retardant, whilst being an inorganic type, non-toxic, environmentally friendly, with low smoke emission and low cost [39,40]. It acts due

to the endothermic dehydration effect, which occurs between 300 °C and 340 °C [41]. Its function in the IFR system is to suppress smoke emissions and cool the surface affected by the fire.

Furthermore, lignosulfonate has numerous advantages, mainly related to its ability to cohere and stiffen a PVAc matrix, as well as to increase its thermal stability [1] through the generation of carbon, which exerts an insulating action on the substrate surface, repressing the flow of oxygen, heat transfer, and the emission of flammable gases [14].

Therefore, this work proposes the development of an intumescent flame retardant and thermal reinforcement bioadditive (IFR), based on a commercial protein matrix from *Saccharomyces cerevisiae* yeast, lignosulfonate, and $Mg(OH)_2$, with the aim of modifying the PVAc adhesive, whose shortcomings are related to its low thermal resistance, which, at the same time, reduces the mechanical strength of the wood-adhesive–wood bond. And thus, it improves the thermal stability and flame retardant properties of the PVAc adhesive (Figure 1).

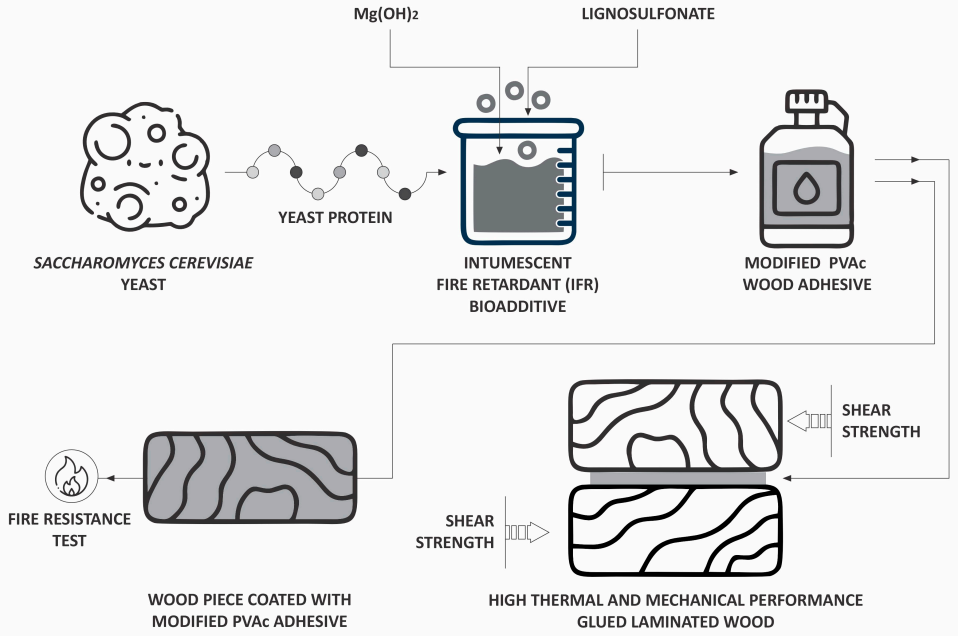

Figure 1. Schematic diagram of the performance of the PVAc adhesive modified with the developed IFR bioadditive.

2. Materials and Methods

2.1. Design and Characterization of the Intumescent Fire-Retardant Yeast–Protein Bioadditive

2.1.1. Elaboration of the IFR Bioadditive

The IFR bioadditive formulations are based on a commercial *Saccharomyces cerevisiae* yeast–protein matrix with a brewing application and lignosulfonate, and an adhesive base elaborated according to Núñez-Decap et al., 2016 [20]. Magnesium hydroxide ($Mg(OH)_2$), in two levels, 4% and 8%, was subsequently added in synthesis at a temperature of 65 ± 1 °C with mechanical agitation of 800 rpm. The experimental design yielded two IFR bioadditive formulations: F1 (4% of $Mg(OH)_2$) and F2 (8% of $Mg(OH)_2$).

Magnesium hydroxide ($Mg(OH)_2$) was obtained from the chemical input supplier, Sigma-Aldrich (Santiago, Chile), whose average particle size corresponds to 20 microns [42]. The lignosulfonate and protein matrix were supplied by the Engineering Products based on Wood and Adhesives Laboratory (PRODIMA-LAB), Universidad del Bío-Bío, Concepción, Chile. Furthermore, the commercial PVAc adhesive for industrial use was provided by a

company in the field of wood adhesives. Its technical characteristics are shown further in Table 6.

2.1.2. Physicochemical and Electrical Characterization

The IFR bioadditive formulations were characterized for their physicochemical and electrical properties, the adhesive viscosity (ASTM D1084-16R21 [43]), pH (ASTM E0070-19 [44]), density (ASTM D1875-03 [45]), electrical conductivity, and solids content (ASTM D1490-01R18 [46]) were evaluated. Three measurements of each property were performed for each IFR bioadditive formulation.

2.1.3. Mechanical and Thermal Characterization

To study the interaction between the bioadditive and the substrate, Dynamic Mechanical Analysis (DMA) was performed through a "three-point bending test" on small-laminated wood specimens, 20 mm long, 5 mm wide, and 1.1 mm thick, bonded with each of the formulations, following the method used in the investigation of Vidal-Vega et al., 2024 [1]. Three measurements of each property were performed for each IFR bioadditive formulation.

Complementarily, the bioadditive formulations were evaluated for their adhesion properties with wood, a relevant property, since it determines the adhesive capacity of the bioadditive and the substrate, as well as its potential compatibility in interactions with the commercial adhesive PVAc. A shear strength test was performed according to ASTM D2339 [47], in specimens with dimensions of 175 mm length, 25 mm width, and 3.2 mm thick, using an Instron universal testing machine. The pressing cycle to achieve adhesion of the veneers through the bioadditive was defined at 12 bar pressures for 6 min at a temperature of 160 °C, with an adhesive grammage of 220 g/m^2 according to Núñez et al., 2016 [20]. The temperatures obtained from the DMA allowed for the establishment of this pressing cycle. Ten specimens were tested for each IFR bioadditive formulation.

According to the requirements of EN 314-1 [48], in the shear strength of veneers (Table 1) values greater than 1.0 MPa do not need a wood failure requirement due to wood tearing, which concerns the joint.

Table 1. Requirement of shear strength and failure values for veneer joints.

Requirements	
Mean Shear Strength fv (MPa)	**Mean Apparent Cohesive Wood Failure (%)**
$0.2 \leq fv < 0.4$	≥80
$0.4 \leq fv < 0.6$	≥60
$0.6 \leq fv < 1.0$	≥40
$1.0 \leq fv$	No requirement

The fire performance of wood pieces coated with the IFR bioadditive formulations was carried out with a volume of 250 mL of each bioadditive formulation. Thus, the fire evaluation was performed on 6 wood pieces for each formulation and 6 standard pieces of natural untreated wood of *Pinus radiata* D. DON with dimensions of 310 mm length, 125 mm width, and 10 mm thick, completely covered by each formulation.

Fire resistance tests were carried out according to ASTM D1360-98 (2011) [49]. The fire resistance test evaluation indicators were defined as carbonization index (%) (Equation (1)) and mass loss (%) (Equation (2)) determined from the tested specimens [50]:

$$CI = ((I_{max} \times \alpha_{max} \times ec)/V_i) \times 100, \quad (1)$$

where CI corresponds to the carbonization index (%); I_{max} corresponds to the maximum length of surface carbonization; α_{max} corresponds to the maximum width of surface char-

ring; ec corresponds to the carbonized thickness; V_i corresponds to the initial volume of the specimen (mm^3).

$$ML = ((P_{at} - P_{dt})/P_{at}) \times 100, \quad (2)$$

where ML corresponds to the mass loss (%); P_{at} corresponds to the weight of the specimen before treatment; P_{dt} corresponds to the weight of the specimen after treatment.

2.1.4. Thermal Characterization by Thermogravimetric Analysis (TGA) and Differential Scanning Calorimetry (DSC)

- Thermogravimetric Analysis (TGA)

The thermogravimetric analysis tests were performed on a Thermal Gravimetric Analyzer (TGA), TA Instruments (TGA), model Q50, located at the Centro de Polímeros Avanzados (CIPA Chile), Concepción, Chile. The test consisted of analyzing the behavior and thermal stability of samples to determine the degradation temperatures and number of residues generated through the Universal Analysis 2000 software. The behavior and thermal stability of the samples were evaluated under a temperature range from 25 °C to 600 °C, using a heating rate of 10 °C/min. Three measurements were performed for each IFR bioadditive formulation.

- Differential Scanning Calorimetry (DSC) Analysis

The DSC analysis was carried out in a differential scanning calorimetry analyzer, PerkinElmer model DSC 6000, located at the Centro de Investigación de Polímeros Avanzados (CIPA Chile), Concepción, Chile. The determination of the transition temperatures and phase changes was performed according to ASTM D3418 [51] in high-pressure capsules. The data acquisition was conducted using the Pyris software platform v.11. The analysis procedure for the samples was carried out by dynamic heating with temperatures from 25 °C to 150 °C, increasing at an incremental rate of 10 °C/min. Three measurements were performed for each IFR bioadditive formulation.

2.2. Preparation of Adhesive Blends Through the Incorporation of Two Bioadditive Formulations to a PVAc Adhesive

The PVAc-bioadditive IFR adhesive blends were prepared with a total mass of 300 g, incorporating concentrations of each bioadditive formulation defined in fractions of 2.5%, 5%, 7.5%, 10%, and 12.5% (*w*/*w*).

The adhesive blends were manufactured by adding the different bioadditive formulations over the PVAc adhesive via permanent agitation at 1100 to 1500 rpm at room temperature (20 ± 5 °C) for 30 min.

According to the preparation methodology and considering the two formulations of the bioadditive, a total of 10 adhesive blends were obtained, which, together with the standard PVAc adhesive, were evaluated for their physicochemical and electrical properties.

2.3. Determination of the Physicochemical and Electrical Properties of PVAc-Bioadditive IFR Adhesive Blends

The physicochemical and electrical properties of the PVAc-bioadditive IFR adhesive blends were performed according to the methods mentioned in Section 2.1.2. Three measurements of each property were performed for each PVAc-bioadditive IFR adhesive blend.

2.4. Evaluation of the Quality of the Adhesive Bond Line on Wood Specimens Glued with PVAc-Bioadditive IFR Adhesive Blends

The quality of the adhesive bond line was evaluated by gluing pieces of dry radiata pine wood, whose moisture content fluctuated between 7% and 10%, and had a basic density between 415 and 552 kg/m^3. The laminated wood pieces were made from two

sheets with dimensions of 19 mm × 100 mm × 450 mm, previously planned to be glued with an adhesive grammage of 220 g/m^2 and an open time of 5 min, and then pressed at 6 kg/cm^2 for 60 min. After pressing, the wood pieces were kept to rest for 7 days under controlled conditions of 25 °C and humidity 8–12%. Then, specimens were extracted for each test: 20 specimens (per test condition) were selected for the shear test, 4 for delamination test (one specimen per joint), and 4 specimens for microscopy (one specimen per joint) per sample. The final dimensions of the specimens for glue line quality testing were as follows: shear test: 36 mm thick, 50 mm wide, and 45 mm long; delamination test: 36 mm thick, 80 mm wide, and 75 mm long; microscopy test: 10 mm thick, 10 mm wide and 10 mm long.

2.4.1. Shear Test at Normal, Elevated Temperature, and Three-Cycle Conditions

The shear strength of the wood specimens glued with the standard PVAc adhesive and the adhesive blends in the three test conditions (normal or dry condition, elevated temperature, and three-cycle) was carried out according to the requirements of ASTM D5751 [52], in accordance with the requirements established in Table 2.

Table 2. Shear strength requirement according to ASTM D5751 Standard.

Performance Classification	Shear Strength (MPa)		Wood Failure (%)	
	Group Average	Individual Minimum	Group Average	Individual Minimum
Cured (dry)	6.69	3.35	30	15
Elevated temperature	4.46	2.23	40	20
Three-Cycle	3.35	1.67	50	25

The shear strength test specimens were evaluated at room temperature (20 ± 5 °C) in an Instron universal testing machine model EMIC 23-100, located at the Laboratory of Engineering Products based on Wood and Adhesives (PRODIMA-LAB), Universidad del Bío-Bío, Concepción, Chile.

2.4.2. Delamination Test

This test was carried out according to ISO 12580 [53], through an accelerated aging cycle in an impregnation cylinder. This cycle includes immersion in water at room temperature and a vacuum of 70 to 85 kPa for 30 min, together with a pressure of 500 kPa for two hours. Once the vacuum–pressure cycle is completed, the samples are taken to an oven at 65 °C and 8% relative humidity, with an air circulation velocity of 2 m/s.

Once the adhesive line quality by shear test and delamination evaluation was completed, five formulations with the highest performance concerning bond line quality were selected.

2.4.3. Study of Adhesive Penetration by Fluorescence Microscopy

The five selected adhesive blends, plus the standard PVAc adhesive, were studied by fluorescence microscopy. Four specimens for microscopy per type of blend were obtained from the wood joints made with the adhesive blends, from which the effective penetration depth (EP) and the average penetration depth (AP) were measured, according to the methodology reported by Vidal-Vega et al. [1].

2.5. Fire Performance Tests on Wood Specimens Coated with Commercial PVAc Adhesive and PVAc-Bioadditive IFR Adhesive Blends

Fire performance tests of the PVAc-bioadditive IFR adhesive blends were performed according to the methods mentioned in Section 2.1.3. The fire evaluation was performed on 6 wood pieces for each blend and 6 standard pieces or natural untreated wood.

2.6. Evaluation of Emissions of Volatile Organic Compounds VOCs from Pure and Modified PVAc Commercial Adhesive Using the IFR Bioadditive: Combustion Method

To facilitate the reading of VOC emissions, the adhesive blends selected were those modified with the formulation of the bioadditive with the highest concentration of elements in its composition (F2), considering the extreme fractions of bioadditive on the commercial adhesive (2.5% and 12.5%). Thus, the adhesive blends to be evaluated were defined as: PVAc-2.5% F2 and PVAc-12.5% F2, which were contrasted with the standard adhesive PVAc and untreated wood.

The test to determine VOCs, through the combustion method, was carried out in wood pieces of dimensions 55 mm width, 70 mm length, and 7 mm thick, under a hood using a cylindrical metal device for laboratory-scale combustion with a volumetric capacity of approximately 864 cm^3, with a side entrance to position the samples to be incinerated. The device was provided with a funnel-shaped metal lid at the top, where the smaller diameter end allowed the smoke outlet and, at the same time, the intake of emissions. The test included the use of an accelerant, 99% pure ethanol, which was applied to the bottom of the device, with a volume of 1.75 mL, and then the specimen was introduced into it. Then, a second 1.75 mL load of ethanol was applied on the upper side of the cylinder, which was distributed towards the rest of the material, thus ensuring the sample ignition.

Thus, the emission measurements were carried out in three instances: the first at the ignition of the wood sample coated with the adhesive blend (time zero); the second in the combustion regime, after 2.5 min of ignition; and finally in the extinction, after another 2.5 min, after the second emission measurement. The total test time was 5 min, with 8 samples, including the duplicate.

The quantification of VOCs was carried out through the use of a thermal desorbed coupled to a Thermal Desorption–Gas Chromatography/Mass Spectrometry (TD-GC/MS) system, located at the Environmental Laboratory of Gases and Biofuels (LAGBIO), University of Talca, Curicó, Chile. Once the specimen was stabilized, emission samples were taken from the smoke outlet. Then, a suction pump (Markes Easy VOC model LP-1200, Markes International GmbH, Offenbach, Germany) was used to extract the gas samples, extracting a quantity of 100 mL through an absorbent tube. Once the gases were adsorbed, desorption of the VOCs was performed using a cold desorption trap. The gases were extracted in Split mode, conducted with helium for 1 min in the heated trap programmed at 300 °C, cooled to 20 °C in the cold trap, then finally heated to 300 °C for 5 min. The VOCs were transferred via a transfer line heated to 200 °C to a column installed in a GC/MS (Thermo Fisher Scientific, model Trace 1300/ISQELTL, Waltham, MA, USA). The GC working conditions for the oven were in Split mode with an operating temperature between 40 °C and 220 °C. Flow rate: 1.2 mL/min; Split ratio: 10 °C/min. The MS detector transfer line temperature was 200 °C while the ion source temperature was set at 250 °C. Qualitative VOC identification was performed using the Chromeleon 7 software package.

2.7. Morphological and Elemental Study by Scanning Electron Microscopy with Energy Dispersive X-Rays (SEM/EDS) of Wood Coated with PVAc Adhesive Unmodified and PVAc Modified with IFR Bioadditive

The morphological study of the carbonized samples under adverse fire conditions (incinerated by the action of an accelerant, 99% pure ethanol), stemming from the evaluation

test of VOCs in combustion, was carried out by means of a Scanning Electron Microscope SEM, model VEGA3 EASYPROBE SBU (TESCAN, Brno, Czech), with an energy dispersive X-ray (EDS), high resolution and an energy range (up to 3 nm at 30 kV), as well as a variable pressure system, for high and low vacuum working modes. This equipment is located at the Advanced Microscopy Center (CMA), Universidad de Concepción, Concepción, Chile.

The study, of the untreated carbonized wood samples and the wood coated with the standard adhesive, for the morphological and elemental study were extracted from the side of the wood specimen, in the direction of the fibers. These were subsequently delimited using a dividing line in a zone of high damage (L) and one of moderate affectation (R), with special attention to the transition area between both zones.

2.8. Statistical Analysis of the Results

The data obtained from the evaluations of the IFR bioadditive formulations and the PVAc-bioadditive IFR adhesive blends were analyzed statistically to establish if there were significant statistical differences between the quantitative characteristics of the samples. The data, with a normal distribution, was analyzed by ANOVA and Fisher's multiple range test (LSD), with a confidence interval of 95%. This analysis was carried out using Statgraphics Centurion XVII 19-X 64 statistical software.

3. Results and Discussion

3.1. IFR Bioadditive Characterization

3.1.1. Physicochemical and Electrical Characterization

The physicochemical and electrical characterization of the IFR bioadditive formulations included the determination of pH, viscosity, density, solids content, and electrical conductivity (Table 3).

Table 3. Average values of bioadditive properties.

ID IFR Bioadditive Formulations	Ph	Viscosity (cP)	Density (g/cm^3)	Solids Content (%)	Electrical Conductivity (mS)
F1	9.33	846.00	1.32	57.40	4.32
F2	9.57	896.67	1.33	62.17	4.54

In general, the average density of the bioadditive formulations was 1.33 g/cm^3. The electrical conductivity was approximately 4 to 5 (mS), without observing important differences between them. In addition, the pH values remained between 9.33 and 9.57, in an alkaline range typical of the base $Mg(OH)_2$ presence.

Viscosity values ranged from 846.00 to 896.67 cP, and solids content was 57.40% to 62.17%.

In terms of these properties, the strength of the adhesive bond tends to decrease when incorporating additives with lower viscosities than the base adhesive (Table 6); however, this property also evidences some degree of compatibility between the different elements that compose the IFR bioadditive formulation [54]. This is because viscosity also depends on the solid content and other components incorporated in the polymeric blend to modify its physicochemical, mechanical, thermal, and other properties [55]. This will be studied by modifying the commercial adhesive according to the quality of the bond line and the penetration of the adhesive. On the other hand, the formulations of the bioadditive presented a solid content, which rose according to the increase in the components of the formulation and reached magnitudes higher than those found in a PVAc adhesive (Table 6), where a higher solids content has a direct relation with the mechanical strength

of the bond [56]. In this regard, the evidence suggests that the reaction of the LS would favor the formation of bonds, for example, hydrogen bonds with the protein, or through other mechanisms, with the different elements of the IFR bioadditive, forming molecules of greater complexity. This is due to the hydrosoluble extremes (sulfonate and carboxylic groups) soluble and water dispersion of this biopolymer, as well as its less polar groups (aromatic and aliphatic), which facilitate the interaction with surfaces of other materials, favoring the formation of interfaces [57,58].

3.1.2. Characterization of IFR Bioadditive Formulations: Dynamic Mechanical Analysis (DMA), Shear Test, and Fire Resistance Test

The average values obtained by the DMA, shear strength and fire resistance test are presented in Table 4.

Table 4. Characterization of IFR bioadditive formulations: dynamic mechanical analysis (DMA), shear test, and fire resistance test.

Test	Property	F1	F2
DMA	E′ Maximum (Pa) Average	$2.041 \times 10^9 \pm 6.69 \times 10^7$	$2.398 \times 10^9 \pm 9.21 \times 10^7$
	T (°C) E′ Maximum Average	122.57 ± 0.41	164.67 ± 1.15
Shear test	Shear strength (MPa)	$0.95^{b} \pm 0.11$	$1.14^{c} \pm 0.15$
Fire resistance test	Mass loss (%) (ML)	$7.52^{a} \pm 0.66$	$10.72^{a} \pm 1.44$
	Carbonization index (%) (CI)	$3.44^{a} \pm 0.89$	$4.46^{a} \pm 1.94$

The results correspond to the mean ± St. Dev. ^{a,b,c} reflects statistically significant differences, according to LSD test with 95% confidence interval (no statistically significant differences between levels sharing the same column or letter). Statgraphics Centurion XVII 19-X 64 software.

The dynamic mechanical analysis (DMA) was performed to observe the wood-bioadditive–wood interaction and the degree of stiffness of the composite material once the bond line had cured. The storage modulus E′ (stiffness) values ranged between 2.041×10^9 and 2.398×10^9 Pa, where the highest magnitude was reached by formulation F2. This rheological behavior could be related to the presence of lignosulfonate and $Mg(OH)_2$ in the formulation, where F2 contains the highest fraction of $Mg(OH)_2$. Magnesium hydroxide has been used to improve thermal resistance and reduce costs in the manufacture of materials such as PVC [59], and as reinforcement in various polymeric matrices [60,61]. Previous studies have highlighted a synergistic relationship between $Mg(OH)_2$ and casein [36], suggesting that yeast protein could form similar structures with $Mg(OH)_2$. Amino acids present in yeast protein, such as aspartic and glutamic acid, are also found in casein, which favors the synergistic reaction [36]. This effect, together with LS as a crosslinker, would explain the increased stiffness observed in the formulations. Thus, the highest magnitude value of E′, of the composite material (wood-bioadditive–wood) is concurrent with the highest concentrations of magnesium hydroxide in the IFR product formulations.

Dynamic mechanical analysis (DMA) not only made it possible to determine the stiffness of the wood-bioadditive–wood bond but also facilitated the definition of a pressing cycle to evaluate the adhesion properties of the PVAc-bioadditive IFR adhesive blends on veneer bonds.

Regarding the shear strength results, the strength values ranged from 0.95 to 1.14 MPa, where formulation F2 presented the highest value. In general, it was observed that the shear strength increased by the higher concentration of $Mg(OH)_2$. Magnesium hydroxide has been used as a filler in PVAc adhesives for wood, improving its mechanical strength and fire-retardant properties. In shear tests, a concentration of 7.5 phr showed the highest strength (1140 N), outperforming pure PVAc adhesive (1027 N), and with $Mg(OH)_2$ acting

as a reinforcing filler. However, at 10 phr, the shear strength decreased [62]. The synergy between magnesium hydroxide and lignosulfonate, with sulfonate and methoxyl groups, enhances the interaction with the adhesive matrix of protein and wood, favoring the formation of cross-linked structures and strong adhesive bonds through hydrogen bridges due to their polarity [1].

In addition, all the joints manufactured with the PVAc-bioadditive IFR adhesive blends presented results of shear strength above the maximum failure requirement value of 0.6 MPa (Table 1), which gives a good clue about the adhesion properties of the product with the wood.

Fire retardancy tests were performed on wood specimens coated with each formulation, in which differences in weight and carbonization of each sample are not significant, since the fire tests did not show statistical variations between the ML and CI indicators in treated wood. However, differences were observed concerning untreated wood, showing that the IFR bioadditive slows combustion (Figure 2). Therefore, both formulations act favorably as passive fire protection products. The presence of the components of the formulations would be acting complementarily, thus, the proteins provide their intrinsic intumescence properties [31,34], magnesium hydroxide, endothermic dehydration that cools the substrate surface [41], and LS contribute to the formation of significant volumes of carbon at high temperatures, coming from the abundant aromatic compounds in its structure [63].

(**a**) (**b**) (**c**)

Figure 2. Uncoated and coated wood specimens with the IFR bioadditive after fire resistance test: (**a**) Uncoated wood; (**b**) Wood coated with IFR F1 formulation; (**c**) Wood coated with IFR F2 formulation.

3.1.3. Thermal Characterization by Thermogravimetric Analysis (TGA) and Differential Scanning Calorimetry (DSC)

Thermal characterization by TGA and DSC of the IFR bioadditive formulations F1 and F2 was also performed for the protein matrix. This was performed to compare the thermal behavior of the bioadditive base concerning the formulations and the effect of $Mg(OH)_2$ on its composition.

- Thermogravimetric Analysis (TGA)

The thermograms show the mass loss curve (Figure 3a) and its derivative (Figure 3b), which identify the thermal peaks associated with the decomposition of the components of each sample as the temperature increases. The maximum points of the derivative correspond to the inflection levels of the mass loss curve, which are marked with segmented red lines.

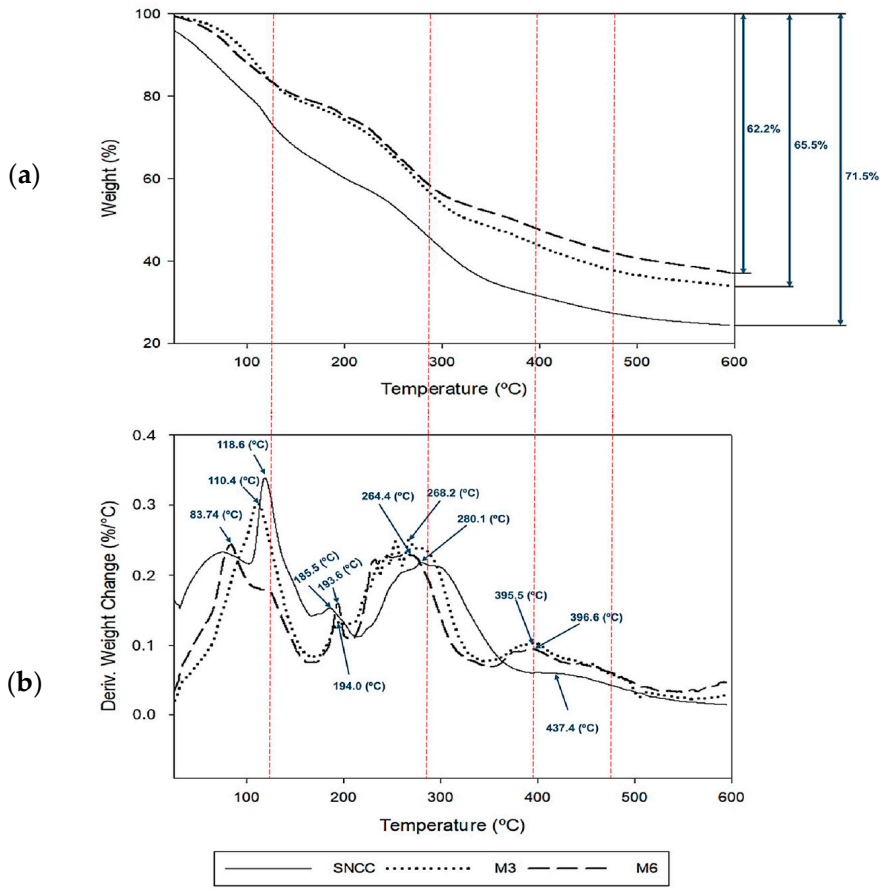

Figure 3. Thermogravimetric analysis (TGA) of formulations F1, F2, and PM: (**a**) Mass loss curve; (**b**) Derivative of mass loss curve.

The mass loss curve shows a first weight drop between 80 °C and 119 °C, due to the evaporation of water in the bioadditive formulations and protein matrix. At temperatures above 100 °C, the protein starts to decompose [9]. Between 186 °C and 194 °C, another mass loss associated with the release of CO and CO_2, typical of organic compounds, is observed [64].

The temperature peak between 260 °C and 280 °C in the thermograms could indicate the decomposition of phosphorus (phosphate) and hemicellulose in protein matrix (PM) crude fiber, with greater intensity in formulations F1 and F2 due to the decomposition of these compounds and the initial reaction of lignosulfonate [65]. Peaks between 395 °C and 437 °C suggest the decomposition of lignin and cellulose in PM crude fiber, with higher intensity in F1 and F2 due to the same elements and the effect of lignosulfonate in a second stage of decomposition [65]. In addition, magnesium hydroxide could undergo physical changes between 340 °C and 490 °C [41,66].

According to Figure 3a, formulation F2 presented the lowest mass loss (62.2%) and the highest residue (37.8%), followed by F1 with 65.5% mass loss and 34.7% residue, and finally PM with 71.5% mass loss and 28.5% residue. The residues correspond mainly to mineral salts, non-nitrogenous compounds (crude fiber), and primarily magnesium hydroxide, which forms magnesium oxide upon degradation [66]. The results coincide with the concentrations of the components of the formulations, with F2 being the most thermally stable due to its higher $Mg(OH)_2$ content, presenting the lowest mass loss.

- Differential Scanning Calorimetry (DSC) Analysis

DSC analysis showed the proteins contained in the PM (Figure 4), presented an exothermic reaction between 27 °C and 30 °C, attributed to temperature-induced molecular interactions, and an endothermic peak at approximately 55 °C, indicating the onset of the denaturation process [67]. On the other hand, formulation F1 reached a maximum Tg of 62 °C and a final Tg of 87.01 °C, with a vitreous-amorphous transition enthalpy of −116.79 mJ. In contrast, formulation F2 exhibited a maximum Tg of 56.82 °C, a final Tg of 88.15 °C, and a transition enthalpy of −224.67 mJ. This suggests that F2 requires more energy to complete the liquid-to-solid state transition, indicating greater thermal stability compared to F1. Table 5 summarizes these key thermal data for both formulations. The vitreous transition temperatures of the F2 formulation are lower than those of F1, indicating that F2 is more reactive and requires less temperature to initiate its exothermic process and interactions between its components. F2 also demands almost twice as much energy as F1 (4% of $Mg(OH)_2$) for the reaction, which correlates with its higher concentration of $Mg(OH)_2$ (8%). This behavior supports the results reported by Uddin et al. (2020) [36], who pointed out a synergistic relationship between proteins and $Mg(OH)_2$. In this study, the presence of LS in the IFR bi-additive formulation should be considered, which would also contribute to the formation of complex structures by releasing energy during intermolecular reactions.

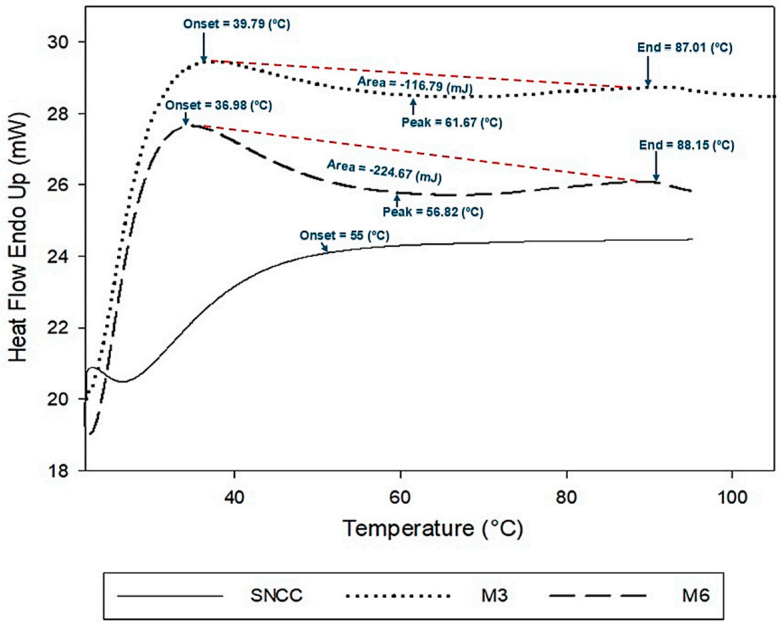

Figure 4. Differential scanning calorimetry (DSC) analysis of F1, F2, and PM formulations. The segmented red lines correspond to the delimitations of the area on the curve associated with the energy released during the DSC test.

Table 5. Thermal points of the IFR bioadditive formulations, in DSC analysis.

Formulation	Tg Initial (°C)	Tg Maximum (°C)	Tg Final (°C)	Energy Released (mJ)
PM	55.00	-	-	-
F1	39.79	61.67	87.01	−116.79
F2	36.98	56.82	88.15	−224.67

Hence, after the thermal evaluation by TGA and DSC of the IFR bioadditive formulations (F1 and F2) concerning the PM, it is possible to establish that the incorporation of LS and $Mg(OH)_2$ improves the thermal stability of the protein itself, providing a better performance against high temperatures.

3.2. Physicochemical and Electrical Properties of PVAc-Bioadditive IFR Adhesive Blends

Table 6 shows the average values of the physicochemical and electrical properties of the modified commercial PVAc adhesive, using the two formulations of the IFR bioadditive, F1 and F2.

Table 6. Physicochemical and electrical properties of the PVAc-bioadditive IFR adhesive blends.

PVAc-Bioadditive IFR Adhesive Blends	pH	Viscosity (cP)	Density (g/cm^3)	Solids Content (%)	Electrical Conductivity (mS)
PVAc	3.26	5823.33	1.12	53	13.22
PVAc-2.5% F1	3.35	3217.67	1.11	53	12.26
PVAc-5% F1	3.56	3243.33	1.01	54	12.19
PVAc-7.5% F1	3.83	3237.67	1.08	55	12.16
PVAc-10% F1	4.25	5493.33	0.97	55	11.78
PVAc-12.5% F1	4.89	5740.00	0.99	56	11.30
PVAc-2.5% F2	3.52	3868.67	1.12	53	12.98
PVAc-5% F2	3.88	4320.00	1.01	54	12.73
PVAc-7.5% F2	4.40	3311.00	0.99	54	11.69
PVAc-10% F2	4.74	6616.67	0.99	54	11.63
PVAc-12.5% F2	6.67	8106.67	1.04	56	11.17

It was observed that by increasing the concentration of the IFR bioadditive formulations in the PVAc adhesive blends, there was a progressive increase in pH and a decrease in electrical conductivity. This effect was more pronounced in the adhesive blends with F2 formulation, which contains a higher proportion of $Mg(OH)_2$, which increased alkalinity and reduced electrical conductivity. $Mg(OH)_2$ is an electrical insulator, with a band gap of 5.7 eV [68], which contributes to this decrease in electrical conductivity, as has also been observed in other $Mg(OH)_2$-modified materials [69]. On the other hand, as was mentioned by Vidal-Vega et al. [1], electrical conductivity is a relevant property, because most of the time wood products bonded with PVAc adhesive are pressed using radiofrequency technology, which accelerates cured and production times [70,71]. So, the idea of measuring this property is to observe how this parameter of the bioadditive could influence the electrical conductivity of the modified adhesive. It was observed that the viscosity of the adhesive blends decreased when incorporating the IFR bioadditive, but when exceeding 10% concentration, the viscosity approached that of the pure PVAc adhesive, especially in the F2 formulation. This decrease is attributed to an inefficient interaction between PVAc and the bioadditive [72], reducing the viscosity at low concentrations. On the other hand, an increase in viscosity upon exceeding 10% bioadditive suggests an increased macromolecular interaction, due to the higher availability of the bioadditive in the system, forming bonds such as "Van der Waals forces" [73] and "hydrogen bridges" [74,75] between the adhesive and the IFR bioadditive, which increases fluid friction and thus viscosity. Finally, the density values of the adhesive blends were close to 1 g/cm^3, without significant variations. As expected, the solids content increased as the concentration of the bioadditive increased, since the blend of the adhesive with the bioadditive incorporated additional

solid elements. The variation in solids content was similar for adhesive blends containing F1 and F2 formulations.

3.3. Adhesive Bond Line Quality on Wood Specimens Glued with PVAc-Bioadditive IFR Adhesive Blends: Mechanical Properties

3.3.1. Shear Strength Test

Table 7 presents the results of shear strength and wood failure under normal, elevated temperature, and three-cycle conditions compared to the requirements of ASTM D5751.

Table 7. Average shear strength and wood failure values of laminated-glued specimens with PVAc-bioadditive IFR adhesive blends in normal, elevated temperature, and three-cycle conditions.

PVAc-Bioadditive IFR Adhesive Blends	Cured (dry) Condition		Elevated Temperature Condition		Three-Cycle Soak Condition	
	Shear Strength (MPa)	Wood Failure (%)	Shear Strength (MPa)	Wood Failure (%)	Shear Strength (MPa)	Wood Failure (%)
PVAc	10.01 ^{bc} ± 1.72	84 ^{bc} ± 16	5.21 ^{a} ± 1.17	50 ^{c} ± 23	8.86 ^{ab} ± 1.53	79 ^{d} ± 30
PVAc-2.5% F1	9.08 ^{bc} ± 2.32	71 ^{b} ± 22	6.84 ^{bc} ± 1.18	50 ^{c} ± 37	8.65 ^{ab} ± 2.30	76 ^{d} ± 19
PVAc-5% F1	10.04 ^{bcd} ± 2.22	83 ^{bc} ± 14	6.50 ^{bc} ± 1.68	44 ^{c} ± 32	7.24 ^{ab} ± 2.73	64 ^{c} ± 23
PVAc-7.5% F1	6.77 ^{a} ± 2.76	55 ^{a} ± 35	5.46 ^{a} ± 1.28	13 ^{a} ± 8	2.74 ^{a} ± 1.40	24 ^{b} ± 15
PVAc-10% F1	8.53 ^{b} ± 2.54	80 ^{bc} ± 20	6.56 ^{bc} ± 1.33	13 ^{a} ± 8	2.04 ^{a} ± 0.93	18 ^{ab} ± 11
PVAc-12.5% F1	9.43 ^{bc} ± 3.20	82 ^{bc} ± 26	8.90 ^{e} ± 2.26	34 ^{bc} ± 28	1.55 ^{a} ± 0.48	10 ^{a} ± 4
PVAc-2.5% F2	11.57 ^{de} ± 2.05	91 ^{c} ± 13	6.49 ^{bc} ± 1.90	36 ^{bc} ± 37	8.76 ^{ab} ± 2.51	82 ^{d} ± 18
PVAc-5% F2	12.21 ^{e} ± 1.80	90 ^{c} ± 11	8.30 ^{e} ± 1.48	75 ^{d} ± 21	11.70 ^{ab} ± 3.18	75 ^{cd} ± 20
PVAc-7.5% F2	10.27 ^{cd} ± 2.97	89 ^{c} ± 10	7.21 ^{cd} ± 1.81	23 ^{ab} ± 27	3.43 ^{a} ± 1.56	29 ^{b} ± 14
PVAc-10% F2	10.14 ^{cd} ± 2.63	80 ^{bc} ± 25	6.19 ^{ab} ± 1.65	38 ^{bc} ± 29	2.10 ^{a} ± 1.57	21 ^{b} ± 16
PVAc-12.5% F2	10.41 ^{cd} ± 2.67	92 ^{c} ± 12	7.92 ^{de} ± 1.49	40 ^{bc} ± 32	3.91 ^{b} ± 2.51	20 ^{ab} ± 17
Requirement	**6.69**	**30**	**4.46**	**40**	**3.35**	**50**

The results correspond to the mean ± St. Dev. ^{a,b,c,d,e} reflect statistically significant differences, according to LSD test with 95% confidence interval (no statistically significant differences between levels sharing the same column or letter). Statgraphics Centurion XVII 19-X 64 software.

In dry conditions, the shear strength of specimens bonded with PVAc-bioadditive IFR adhesive blends ranged from 6.77 MPa to 12.21 MPa. The PVAc-5% F2, PVAc-2.5% F2, and PVAc-12.5% F2 blends exhibited the highest strengths, outperforming the standard PVAc adhesive by 22%, 16%, and 4%, and exceeding the 6.69 MPa requirements of ASTM D5751 by 83%, 73%, and 56%, respectively. Wood failure ranged from 55% to 92%, being higher in the same mixes, with increases of 10%, 8%, and 7% over the standard adhesive and exceeding the standard requirement by more than 200% (30%).

The results indicate that the modified adhesive with IFR bioadditive provided similar or superior shear strength and wood failure to the standard adhesive, and it was significantly higher than the required by the standard. In particular, the F2 formulation at low concentrations (2.5% and 5%) showed significantly higher strength and better wood failure than the commercial PVAc adhesive. This suggests that less intervention in the commercial adhesive optimizes its mechanical properties. However, an excess of bioadditive can generate brittleness due to stresses, defects, or excess additives that exceed the reaction capacity of the polymer matrix [59].

The bioadditive with high concentrations of $Mg(OH)_2$ (formulation F2) significantly strengthened the adhesive system, in line with the study of Dasaesamoh et al. (2021) [62] on $Mg(OH)_2$-reinforced PVAc. This showed improvements in shear load carrying capacity, reaching its maximum at 7.5 phr, outperforming the standard adhesive by 11%. However,

higher concentrations (10 phr) reduced the reinforcing capacity due to inefficient interactions between $Mg(OH)_2$ and the polymer. This highlights the importance of determining specific limits in the modification of PVAc adhesives since small amounts of additive can achieve significant improvements, but excess amounts can impair their mechanical properties [76,77].

Under elevated temperature conditions, the shear strength of the samples ranged from 5.21 MPa to 8.90 MPa. The PVAc-12.5% F1, PVAc-5% F2, PVAc-12.5% F2, and PVAc-2.5% F1 adhesive blends showed the highest strengths, exceeding the standard adhesive by 71%, 59%, 52%, and 31%, respectively. They also exceeded the ASTM D5751 requirements (4.46 MPa) by 100%, 86%, 76%, and 53%. As for wood failure, values ranged from 13% to 75%, with the highest values for PVAc-5% F2, which exceeded the standard by 50%, and PVAc-2.5% F1, which equaled the standard result. Samples PVAc-5% F2 and PVAc-2.5% F1 exceeded the standard requirement for wood failure (40%) by 88% and 25%, respectively, while samples PVAc-5% F1 and PVAc-12.5% F2 met the established limit.

The IFR bioadditive, composed of a PM, $Mg(OH)_2$, and LS, improved the thermal stability and mechanical properties of the PVAc adhesive, especially in adhesive blends such as PVAc-5% F2. This increased the bond stiffness under high temperatures (104 °C for 6 h), exceeding the performance of the standard adhesive. However, this reinforcing effect may have reduced the ductility and penetration of the adhesive blend, resulting in rips lower than those required by the standard. A similar study on PVC modified with $Mg(OH)_2$-lignin showed an increase in the stiffness and thermal stability of the polymer with higher concentrations of the additive, improving its resistance to thermal decomposition compared to pure PVC [78].

In the evaluation of shear strength under three-cycle conditions, values ranged from 1.55 MPa to 11.70 MPa. The highest strengths occurred in the PVAc-5% F2, PVAc-2.5% F2, and PVAc-2.5% F1 blends, with only PVAc-5% F2 exceeding the strength of the standard adhesive by 32%. These joints also exceeded the values required by ASTM D5751 (3.35 MPa) by 249%, 161%, and 158%, respectively. For wood failure, values ranged from 10% to 82%, with the PVAc-2.5% F2, PVAc-2.5% F1, and PVAc-5% F2 blends having the highest failures (82%, 76%, and 75%). These samples also exceeded the wood failure requirement (50%) of ASTM D5751, with increases of 64%, 52%, and 50%, respectively, but only PVAc-2.5% F2 showed a 4% increase over the standard.

In the three-cycle condition, the samples were subjected to immersion in water at room temperature for 4 h, followed by 19 h at 43 °C, repeating this process three times. PVAc adhesive, a thermoplastic polymer with a low vitreous transition temperature (Tg) near 30 °C [1], is sensitive to moisture and high temperatures [74]. During cycling, the polymer fluence could have favored a good mechanical anchorage between the adhesive and the wood. The bonds with the bioadditive-modified adhesive (2.5% and 5% in F2) showed higher stiffness and ductility, reaching shear strengths and wood failure close to or higher than the standard adhesive. However, samples with concentrations higher than 7.5% bioadditive (F1 and F2) showed poor performance, with failures outside the limits required by the standard. This negative performance is attributed to the embrittlement of the glue line due to the excessive presence of additive, which generates internal tensions, leading to defects and discontinuity at the interface [59], emphasized by humidity and temperatures higher than the Tg of the adhesive. Consequently, this results in joints with poor mechanical performance.

3.3.2. Delamination of Wood Joints and Penetration of Modified Commercial PVAc Adhesive Using IFR Bioadditive

Delamination is a defect in the adhesive bond caused by the weakening of the glue line due to aging, exposure to moisture and temperature, or factors such as inadequate

substrate preparation, grammage, properties of the adhesive resin, and incompatibility of the adhesive with the conditions of use [79].

The results of the average delamination in wood specimens glued with PVAc-bioadditive IFR adhesive blends (Figure 5a) showed variations between 0% and 70%. The pure PVAc adhesive presented the lowest delamination (0%), followed by the PVAc-2.5% F1 (3%) and PVAc-5% F2 (5%) adhesive blends, meeting the requirement $\leq$ 5%, according to ISO 12580. Based on the statistical analysis, no statistically significant differences were found between these samples.

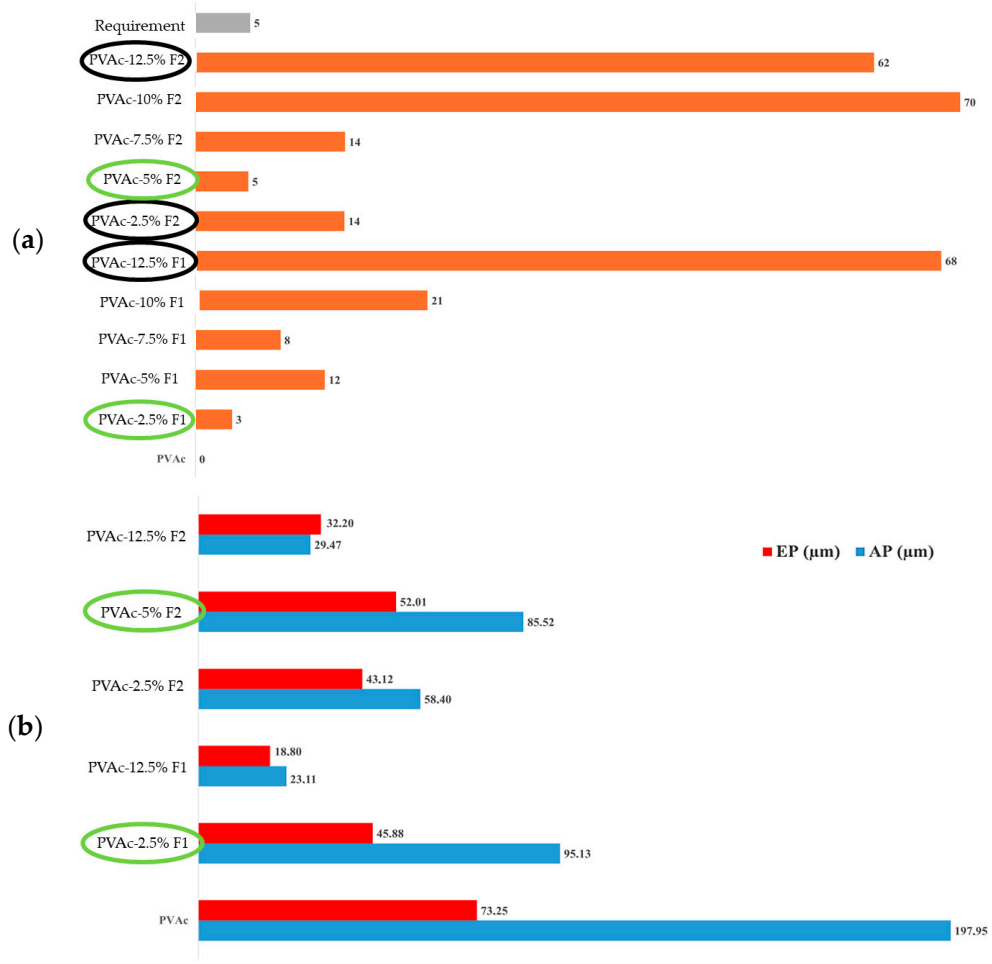

Figure 5. Quality of the bonding line: (**a**) Delamination (%) of all glued-laminated timber joints; (**b**) Penetration (µm), of the five selected PVAc-bioadditive IFR adhesive blends.

According to the results obtained by the shear test and delamination evaluation, five formulations with the highest performance concerning bond line quality were selected to measure the adhesive penetration and fire resistance, which were: PVAc-2.5% F1; PVAc-12.5% F1; PVAc-2.5% F2; PVAc-5% F2; PVAc-12.5% F2, and as a comparative base, the standard PVAc adhesive.

It was found that the effective penetration depth (EP) and average penetration depth (AP) values ranged between 18.80 and 73.25 µm and 23.11–197.95 µm, respectively. The highest EP and AP values were observed in joints with standard PVAc adhesive, followed by PVAc-5% F2 and PVAc-2.5% F1 adhesive blends, meeting the ISO 12580 standard (delamination $\leq$ 5%). On the other hand, the lowest penetrations and highest delamination (68% and 62%) occurred in joints with PVAc-12.5% F1 and PVAc-12.5% F2 (Figure 5b).

The low penetration depth in adhesive blends with higher bioadditive concentration could be due to their higher viscosity, as in the 12.5% F2 formulation (8106.67 cP) compared

to the standard adhesive (5823.33 cP). This is reflected in the morphology of the glue lines: the PVAc standard adhesive showed higher penetration into the substrate (Figure 6a), while PVAc-12.5% F2 showed the lowest penetration (Figure 6b).

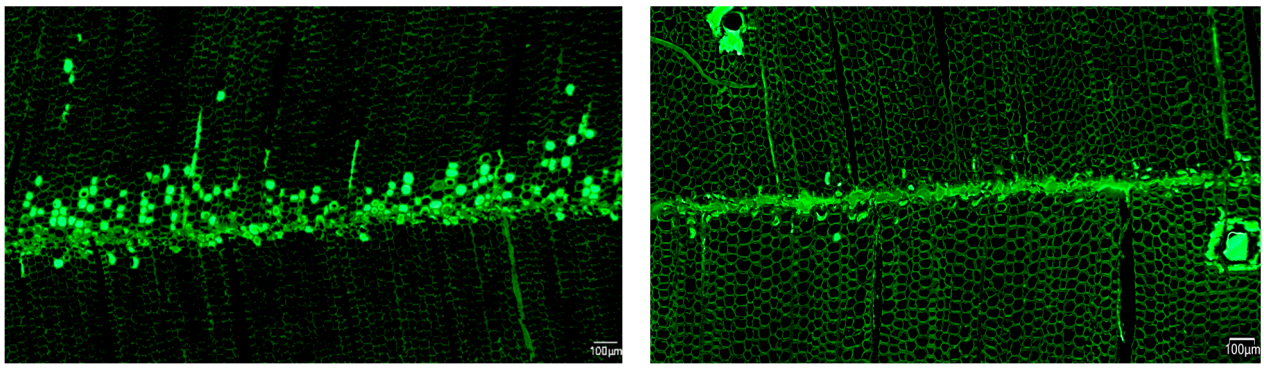

(**a**) (**b**)

Figure 6. Adhesive penetration and glue line morphology: (**a**) PVAc adhesive line; (**b**) PVAc-12.5% F2 adhesive line.

A greater penetration of the adhesive into the pore spaces of the wood such as lumens and cell walls favors the formation of solid bonds between the resin and the substrate, which improves the quality and strength of the adhesive bond [80]. Adhesive penetration depends on factors such as resin properties, wood characteristics, and gluing process conditions [81]. Adhesive viscosity is key: high viscosity limits penetration, while low viscosity can cause over-penetration, affecting the adhesive line's quality and the bond's mechanical performance [82,83]. In addition, high concentrations of bioadditive result in stiff but brittle bonds, with weak adhesion that can result in significant delamination.

3.4. Fire Performance of Wood Parts Coated with PVAc-Bioadditive IFR Adhesive Blends

Table 8 and Figure 7 show the fire performance, mass loss, and carbonization index results of the specimens coated with five PVAc-bioadditive adhesive blends selected and evaluated as coatings on wood pieces. We also included specimens of untreated wood and wood treated with pure or standard PVAc adhesive.

Table 8. Average mass loss and carbonization index values in wood pieces coated with PVAc-bioadditive IFR adhesive blends.

PVAc-Bioadditive IFR Adhesive Blends	Mass Loss (%)	Carbonization Index (%)
Untreated	83.07 ^{d} ± 3.71	77.62 ^{c} ± 6.21
PVAc	10.24 ^{bc} ± 0.98	13.18 ^{b} ± 13.85
PVAc-2.5% F1	9.28 ^{bc} ± 0.99	4.31 ^{ab} ± 1.00
PVAc-12.5% F1	7.81 ^{c} ± 1.49	3.76 ^{ab} ± 0.70
PVAc-2.5% F2	10.79 ^{ab} ± 0.78	3.11 ^{a} ± 0.91
PVAc-5% F2	10.53 ^{c} ± 1.24	5.48 ^{ab} ± 0.55
PVAc-12.5% F2	6.10 ^{a} ± 2.30	3.89 ^{ab} ± 1.07

The results correspond to the mean ± St. Dev. ^{a,b,c,d} reflect statistically significant differences, according to LSD test with 95% confidence interval (no statistically significant differences between levels sharing the same column or letter). Statgraphics Centurion XVII 19-X 64 software.

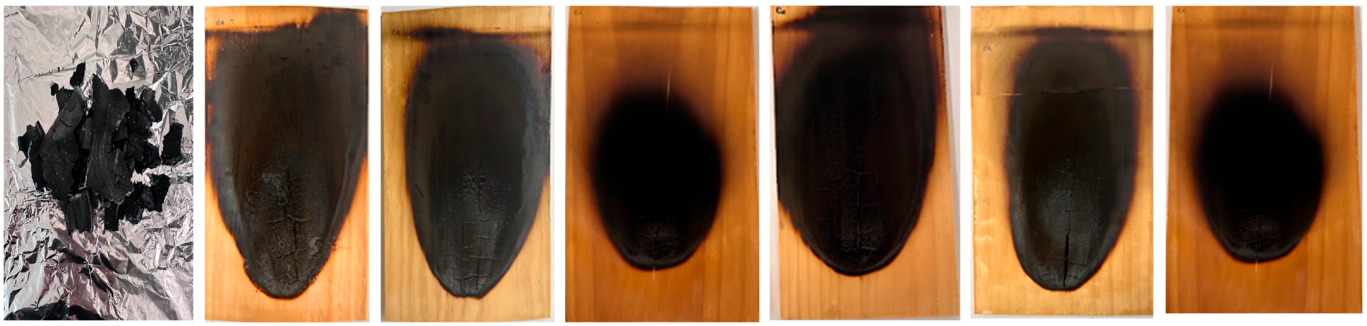

(**a**) (**b**) (**c**) (**d**) (**e**) (**f**) (**g**)

Figure 7. Uncoated and coated wood specimens with the IFR bioadditive after fire resistance test: (**a**) Uncoated wood; (**b**) Wood coated with PVAc; (**c**) Wood coated with PVAc-2.5% F1; (**d**) Wood coated with PVAc-12.5% F1; (**e**) Wood coated with PVAc-2.5% F2; (**f**) Wood coated with PVAc-5% F2; (**g**) Wood coated with PVAc-12.5% F2.

In general, the mass loss of the wood pieces coated with the adhesive blends and tested in a fire chamber ranged from 6.10% to 83.07%. Likewise, the carbonization index ranged from 3.11% to 77.62%. The lowest mass loss values were 6.10% and 7.81% for the wood pieces treated with the PVAc-12.5% F2 and PVAc-12.5% F1 adhesive blends, respectively. On the other hand, the lowest magnitudes of the carbonization index were presented in wood pieces treated with the adhesive blends PVAc-2.5% F2 and PVAc-12.5% F1, with values of 3.11% and 3.76%, respectively.

The statistical analysis showed a significant difference in mass loss between the wood pieces coated with the PVAc-12.5% F2 adhesive blend and those treated with the standard adhesive, as well as those not coated. As for the carbonization index, a significant difference was observed between the pieces treated with the PVAc-2.5% F2 adhesive blend, and those coated with the pure PVAc adhesive, as well as with the untreated pieces.

The results of the fire resistance tests indicate that the PVAc-12.5% F2 and PVAc-2.5% F2 adhesive blends protect wood better against fire than the unmodified PVAc adhesive, according to the mass loss and carbonization index indicators. ML is a more accurate indicator that confirms the effectiveness of the IFR bioadditive, which includes LS and $Mg(OH)_2$. In addition, the higher concentration of $Mg(OH)_2$ in the F2 formulation was crucial to improve the fire performance, which is in agreement with previous research that showed that the combination of $Mg(OH)_2$ and lignin thermally strengthens the materials, highlighting the effect of $Mg(OH)_2$ on thermal stability [84].

3.5. Determination of VOC Emissions in the Combustion of Wood Coated with Unmodified and Modified PVAc Adhesive Using the IFR Bioadditive Formulations

It is important to remember that dry wood (8 to 12% moisture content) and untreated wood react with fire mainly because of the carbohydrates that compose it (65 to 75%) [85], whose chemical structure is based on compounds of hydrogen, oxygen, and carbon, highly flammable and typical of organic materials [86], considering that volatile organic compounds (VOCs) emissions increase with temperature [87].

Table 9 summarizes the VOCs detected in the different stages of combustion (ignition, regime, and extinction). Thity-nine VOCs were identified, with aliphatic and aromatic hydrocarbons predominating, followed by amino acids and carboxylic acids. In addition, 12 compounds were found, possibly derived from the high-temperature reaction (combustion) between the functional groups of these families and other elements of the PVAc-bioadditive IFR adhesive blends.

Table 9. Summary of compounds detected by thermal desorption–gas chromatography/mass spectrometry (TD-GC/MS). Measurement of emissions at ignition, regime, and extinction.

Family	Compound Name (Formula)	Ignition				Regime				Extinction			
		1	2	3	4	1	2	3	4	1	2	3	4
Hydrocarbons	Pentane, 3-methyl- (C_6H_{14})				X								X
	n-Hexane (C_6H_{14})	X			X								X
	Cyclopentane, methyl-(cycloethane) (C_6H_{12})	X											
	Octane, 3-methyl-(alkane) (C_9H_{20})	X											
	Butane, 2,2-dimethyl-(alkane) (C_6H_{14})												X
	Nonane(alkane) (C_9H_{20})	X											
	Butane(alkane) (C_4H_{10})									X			
	Cyclooctane, 1-methyl-3-propyl-(cycloalkane) ($C_{12}H_{24}$)	X											
	Cyclohexane, 1,1,2,3-tetramethyl-(cycloalkane) ($C_{10}H_{20}$)	X											
	1,3-Cyclopentadiene, 5-(1-methylethylidene)-(cyclopentadiene) (C_8H_{10})				X								
	Ethylbenzene (aromatic H.) (C_8H_{10})				X								
	p-Xylene (aromatic H.) (C_8H_{10})				X								
	Benzene (aromatic H.) (C_6H_6)	X	X	X	X	X	X	X	X	X	X	X	X
	Toluene (aromatic H.) (C_7H_8)	X											
	Ethylbenzene (aromatic H.) (C_8H_{10})				X								
Aldehyde	Furfural ($C_5H_4O_2$)									X			
	Butanal, 3-methyl- ($C_5H_{10}O$)				X								
	Pentadecanal- ($C_{15}H_{30}O$)												X
	2-Formylhistamine (aminoderivado) ($C_6H_9N_3O$)								X				
Amino	3-Amino-2-oxazolidinone (cetone) ($C_3H_6N_2O_2$)											X	
	Ethanamine, 2-propoxy-(eter) ($C_5H_{13}NO$)			X				X					
	$C_4H_{10}N_2$				X								
	dl-Alanine (aminoacid) ($C_3H_7NO_2$)				X								
	$C_3H_7NO_2$												X
Carboxylic acid	Acetic acid ($C_2H_4O_2$)						X				X		
	Acetic acid, oxo-, methyl ester(esterified) ($C_3H_4O_3$)												X
	Acetic acid, oxo- ($C_2H_2O_3$)												X
Epoxide (ethoxyuran)	2,3-Epoxybutane (C_4H_8O)					X							
Oxetane	2-Ethyl-oxetane ($C_5H_{10}O$)							X					
Furanoid	Furan, 2-methyl- (C_5H_6O)									X			
Cyclosiloxane	Cyclotrisiloxane, hexamethyl- ($C_6H_{18}O_3Si_3$)				X						X		
Nitroalkane	Butane, 2-nitro- ($C_4H_9NO_2$)			X									
Anhydride-acid (pyruvic acid)	Acetic acid, anhydride with formic acid ($C_3H_4O_3$)			X									
Carboxylic acid ester (dibutyl phthalate)	1,2-Benzenedicarboxylic acid, bis (2-methylpropyl) ester ($C_{16}H_{22}O_4$)			X									
Ether–alkyl	Propane, 1-(ethenyloxy)-2-methyl- ($C_6H_{12}O$)											X	
Carboxylic acid salt	Ammonium acetate ($C_2H_7NO_2$)											X	
Nitroalcohol (ethylnitrate)	Ethanol, 2-nitro- ($C_2H_5NO_3$)								X				
Alcohol-amine	1-Pentanol, 4-amino- ($C_5H_{13}NO$)								X				
Ester	Ethyl Acetate ($C_4H_8O_2$)												X

1: Untreated; 2: PVAc standard; 3: PVAc-2.5% F2; 4: PVAc-12.5% F2; X corresponds to the VOCs found in each combustion sample.

In the combustion test, it was observed that the greatest quantity and variety of VOCs were emitted during the ignition (22 VOCs) and extinction (17 VOCs) stages when large volumes of carbon monoxide (CO) and VOCs are generated. This is a state that decreases with the ignition and permanence of the flame, which is why, during the regime or combustion in development, the occurrence of these decreased notably (8 VOCs) [88]. Thus, the beginning and end of combustion are the most critical stages from the environmental and public health point of view in fire-related incidents.

Consequently, the highest amount of aliphatic and aromatic hydrocarbons was observed during the ignition stage in untreated wood, which presented emissions of ethylbenzene, p-Xylene, benzene, and toluene, which are all VOCs classified as carcinogenic [89,90]. In the wood specimens coated with the PVAc- 12.5% F2 adhesive blend, the presence of ethylbenzene was also found in the ignition. At this stage, the first appearance of amino groups was observed from the wood specimens coated with the adhesive blends PVAc-12.5% F2 and PVAc-2.5% F2, probably caused by the decomposition of the protein-based IFR bioadditive at a high temperature. VOC ethanamine could have been originated from the transformation of the carboxylic group of valines into an alcohol by reacting with a reducing compound present in the system [91]. Cyclosiloxane, nitroalkane, anhydride-acid (pyruvic acid), and carboxylic acid ester compounds were also detected. Cyclosiloxane, formed by silicon and oxygen, could have been generated by the presence of silica in the PVAc adhesive to improve its physical mechanical performance since it was found in both the modified and unmodified samples [92]. The nitro groups come from the protein matrix of the IFR bioadditive, while the anhydro-acid is related to the decomposition of the bioadditive during combustion, possibly by yeast proliferation [93,94]. The carboxylic acid ester, classified as a possible carcinogen [95], may be related to the composition of the commercial PVAc adhesive.

In the combustion regime stage, the emission of aromatic hydrocarbons (such as benzene), typical of wood combustion [88,96], as well as cyclic ethers (oxetane and epoxide), which can be formed when the temperature of the combustion process is reduced [97], was observed. In addition, the detected traces of alcohol-amine probably result from the reaction between alcohol compounds and amine groups on the IFR bioadditive protein during combustion [98]. This VOC was found in the specimens coated with PVAc 12.5% F2.

In the extinction stage, the observed emissions corresponded to aliphatic and aromatic hydrocarbons (such as benzene), aromatic hydrocarbon–amine (benzene–amine), aldehyde group compounds, amino, furanoid, cyclosiloxane, ether–alkyl, carboxylic acid salt, and ester. The presence of furanoid VOC could be due to the hydrogenation of furfural, present in lignocellulosic biomass (wood), during the combustion process [99]. Ether–alkyl, the base component of PVAc adhesive [100], was identified as part of the polymeric base of the adhesive. The carboxylic acid salt (ammonium acetate) was formed by a reaction between ammonia and acetic acid [101]. The ammonia comes from the decomposition of *S. cerevisiae* yeast proteins at high temperatures, which was expected considering that the design of the bioadditive is based on the definition of an intumescent product [13], while the acetic acid could have originated from commercial adhesive or wood, as a result of the cleavage of the acetyl groups of hemicellulose [102].

Summarizing, the most relevant aromatic hydrocarbon for its carcinogenic effects was benzene, present in all stages of combustion. It was observed that its concentration decreased in the regime stage, as the concentration of the bioadditive in the blend with the PVAc adhesive increased. The relative intensity of benzene in the samples was as follows: untreated wood 76%, coated with pure PVAc 65%, with PVAc-2.5% F2 12%, and with PVAc-12.5% F2 4%. It was noted that benzene comes from the intrinsic composition of the wood [88,96], not from the pure PVAc or PVAc-bioadditive IFR adhesive blends.

3.6. Morphology and Elemental Analysis of Wood Samples Coated with PVAc Adhesive Unmodified and PVAc-Bioadditive IFR Adhesive Blends, by Scanning Electron Microscopy with Energy Dispersive X-Rays (SEM/EDS)

The same pieces of wood subjected to combustion for the evaluation of VOCs were studied by scanning electron microscopy (SEM).

3.6.1. Morphological Evaluation of Treated and Untreated Wood Pieces by SEM

Figure 8 shows the study area analyzed by SEM, divided into left (L), severely carbonized area, and right (R), moderately affected area. A transition zone with topographic changes in the surface of the material is observed above the dividing line.

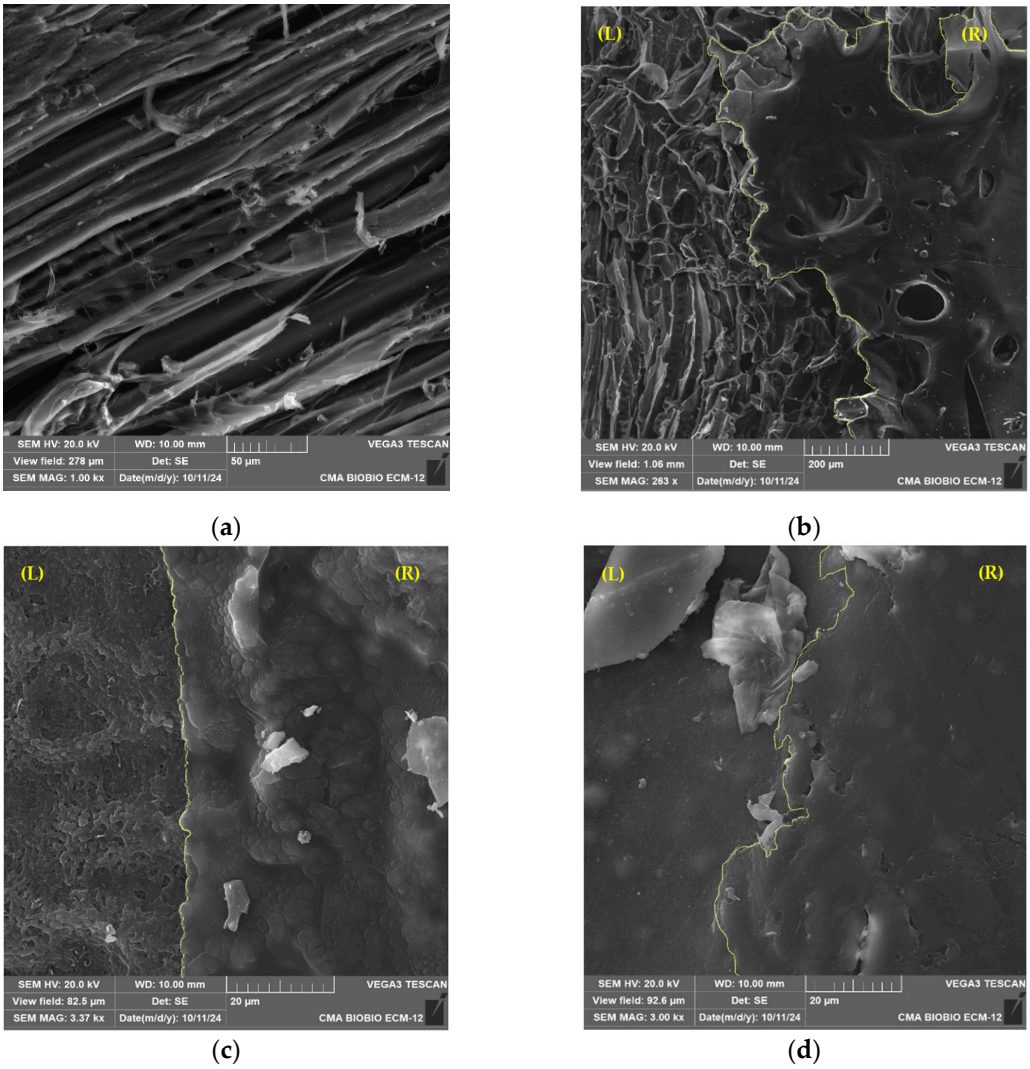

Figure 8. Surface morphology of the samples studied: (**a**) Untreated wood; (**b**) Wood coated with PVAc (standard); (**c**) Wood coated with PVAc-2.5% F2; (**d**) Wood coated with PVAc-12.5% F2.

Figure 8a shows the untreated wood affected by the fire, with the lifting and tearing of tissues, severe exposure of pits in the tracheid, and total damage to its internal structure. The uncoated specimens disintegrated almost completely, showing significant weight loss and deep fractures from the ends toward the center.

Figure 8b shows the wood coated with PVAc adhesive. In area L, severe damage is observed with significant cracks, affecting both the exterior and interior of the sample. In area R, the adhesive layer shows drastic erosion due to the high temperatures, causing internal damage to the wood. Although the adhesive offers some surface protection, in area L, the structural damage is comparable to that of the untreated wood (Figure 8a).

Both Figure 8a,b evidence an amorphous structure of the carbon generated after combustion, with corridors and open spaces that facilitated heat transfer to the interior due to the high availability of oxygen [103]. Consequently, an uncoated wood produces a porous and light carbon that accelerates the release of CO and CO_2, increasing the spread of fire [104].

Figure 8c shows wood coated with the PVAc-2.5% F2 adhesive blend. In zone L, the carbonized area presents a fine and homogeneous porosity, without damaged cellular structures, indicating the formation of thermal insulating carbon that stopped combustion. In zone R, a flaky surface attributed to bubbles formed in the coating through the emission of volatile compounds and water vapor during thermal decomposition is observed [102]. This coating generated a kind of carbon foam that slowed down and stopped the advance of the fire.

Finally, Figure 8d shows the wood coated with the PVAc-12.5% F2 adhesive blend, where areas L and R present similar surfaces. In L, traces of the coating are observed, while in R there is moderate lifting covering the carbonized wood. This sample suffered less damage than the previous ones, forming a compact carbon that limited combustion. The higher efficiency is mainly attributed to the high concentration of $Mg(OH)_2$ (F2) in the blend, which, when interacting with phosphorus compounds contained in the protein matrix, generated an intumescent and dense carbon blocking heat transfer and suppressing combustion and smoke emission [60,105].

3.6.2. Elemental Analysis, by SEM/EDS, of the Studied Surface of One Sample

Figure 9a shows the original image used for the elemental mapping, the result of which is presented in Figure 9b, and the spectrum obtained in Figure 9c. This mapping identified the distribution of elements on the surface of wood coated with PVAc-12.5% F2 after combustion, previously analyzed morphologically in Figure 8d.

SEM/EDS mapping showed a homogeneous distribution of the bioadditive in the adhesive blend, above the substrate surface, with no specific areas of concentration associated with pigmentations defined for each identified element, unlike findings reported in previous studies [106,107].

Elemental analysis identified carbon (C), oxygen (O), nitrogen (N), aluminum (Al), chlorine (Cl), magnesium (Mg), sodium (Na), and phosphorus (P). The main components of wood are C, O, and N, in mass concentrations of 58%, 36%, and 2.7%, respectively. Nitrogen comes from wood, while Mg (0.6%) and Na (0.3%) are associated with minerals from yeast protein matrix and IFR bioadditive. Phosphorus (0.2%) comes from the protein matrix, and Al (0.6%) and Cl (0.9%) are attributed to aluminum chloride ($AlCl_3$), regularly added in PVAc, used to increase the consistency, viscosity, moisture, and temperature resistance, of the PVAc adhesive, in addition with other crosslinking agents, to improve its physical, mechanical and thermal performance [108,109].

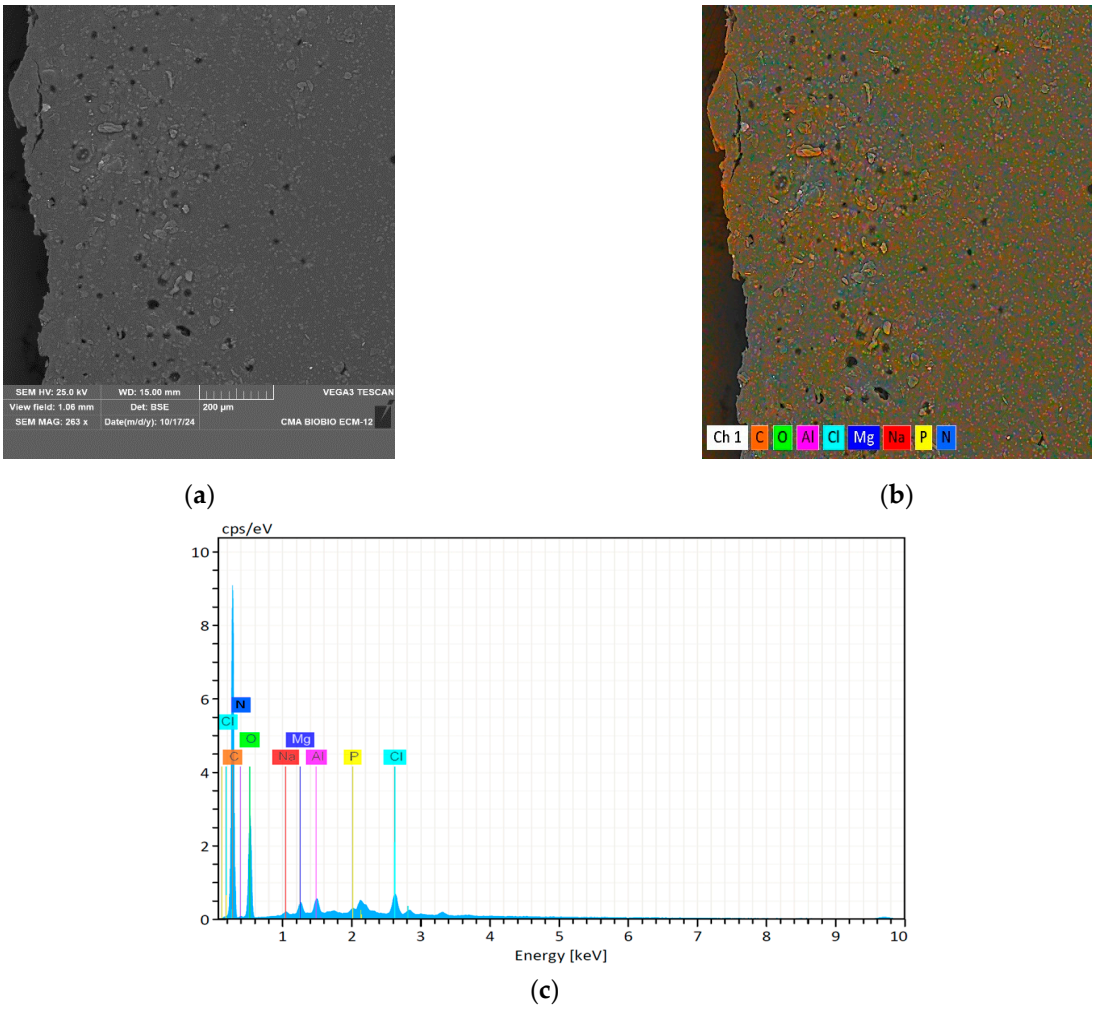

Figure 9. (**a**) Original SEM image of the sample; (**b**) EDS elemental mapping image; (**c**) SEM/EDS elemental spectra analysis of the sample.

4. Conclusions

1. From the development of IFR bioadditive formulations and their physicochemical and electrical evaluation, dynamic mechanical analysis (DMA), shear strength, and fire resistance, it was established that both formulations F1 and F2 were able to modify the commercial PVAc adhesive, although the thermal evaluation (TGA and DSC) of both samples showed that the formulation F2 was the most thermally stable since this formulation contains the highest concentration of $Mg(OH)_2$.
2. From the modified PVAc adhesive blends, the 2.5% F1 and 5% F2 PVAc-bioadditive IFR adhesive blends have been selected, based on the evaluation of mechanical properties. According to the standard requirement, the results of shear test of the elevated temperature condition were 7 MPa and 8 MPa of shear strength, respectively. Additionally, the wood failure results were 50% and 75%, respectively, with the highest deep penetration of the adhesive over the substrate. In addition, according to the delamination standard requirement, the results were 3% and 5%, respectively. On the other hand, according to an intumescent flame-retardant application, the sample 12.5% F2 PVAc-bioadditive IFR adhesive blend had been selected (fire test: 6.10% of mass loss and 3.89% of carbonization index). It can be concluded that it is possible to develop a bioadditive capable of improving the thermal properties of a PVAc adhesive, through the action of lignosulfonate, as a cohesive reinforcement of its polymeric structure, and microbiological protein from commercial yeast

S. cerevisiae and magnesium hydroxide ($Mg(OH)_2$). These are agents that enhance the binder-intumescent properties of the adhesive and act synergistically to improve the performance of PVAc adhesive against high temperatures and fire.

3. Given the decrease in relative intensity associated with the identification of benzene, for example, in combustion, it can be concluded that the bioadditive is capable of masking or encapsulating this type of VOC during the regime stage. Furthermore, VOC emissions with high toxic potential (aromatic hydrocarbons, such as benzene, toluene, p-xylene, among others) correspond to the substrate (wood) and not to the adhesive modified by means of the IFR bioadditive.

Biological materials, such as the bioadditive, would offer the opportunity to decrease the partial or total CO_2 load during its life cycle. In this case, a biological base of yeast protein was established for the elaboration of this bioproduct to maintain the innocuous characteristics of the PVAc adhesive, when modified with it. Undoubtedly, biological materials are a promising alternative in the development of products that are more responsible for the environment and human beings' health.

Author Contributions: Conceptualization, M.V.-V., M.N.-D. and D.H.-E.; methodology, M.V.-V., M.N.-D., D.H.-E. and A.F.-P.; software, M.V.-V.; validation, M.V.-V., M.N.-D. and D.H.-E.; formal analysis, M.V.-V.; investigation, M.V.-V.; resources, M.V.-V., M.N.-D., D.H.-E. and A.F.-P.; data curation, M.V.-V.; writing—original draft preparation, M.V.-V.; writing—review and editing, M.V.-V.; visualization, M.V.-V.; supervision, M.V.-V.; project administration, M.V.-V.; funding acquisition, M.V.-V. All authors have read and agreed to the published version of the manuscript.

Funding: This research received no external funding. The APC was funded by Centro Nacional de Excelencia para la Industria de la Madera (CENAMAD)—ANID BASAL FB210015.

Institutional Review Board Statement: Not applicable.

Informed Consent Statement: Not applicable.

Data Availability Statement: This work information and data are managed by the corresponding author, whose dissemination is restricted due to privacy issues.

Acknowledgments: The authors thank the Universidad del Bío-Bío, Wood and Adhesive Engineering Products Laboratory (PRODIMA-LAB), belonging to the Department of Civil and Environmental Engineering at the Universidad del Bío-Bío, Concepción, Chile, and Centro Nacional de Excelencia para la Industria de la Madera (CENAMAD), Santiago, Chile—ANID BASAL FB210015.

Conflicts of Interest: The authors declare no conflicts of interest.

References

1. Vidal-Vega, M.; Núñez-Decap, M.; Hernández-Durán, J.; Catricura-Muñoz, P.; Jara-Briones, C.; Moya-Rojas, B.; Opazo-Carlsson, C. Comparative Study of Carbon Nanotubes and Lignosulfonate as Polyvinyl Acetate (PVAc) Wood Adhesive-Reinforcing Agents. *Appl. Sci.* **2024**, *14*, 365. [CrossRef]
2. Petković, G.; Vukoje, M.; Bota, J.; Pasanec Preprotić, S. Enhancement of Polyvinyl Acetate (PVAc) Adhesion Performance by SiO_2 and TiO_2 Nanoparticles. *Coatings* **2019**, *9*, 707. [CrossRef]
3. Jiang, W.; Tomppo, L.; Pakarinen, T.; Sirviö, J.; Liimatainen, H.; Haapala, A. Effect of Cellulose Nanofibrils on the Bond Strength of Polyvinyl Acetate and Starch Adhesives for Wood. *BioResources* **2018**, *13*, 2283–2292. [CrossRef]
4. Khan, U.; May, P.; Porwal, H.; Nawaz, K.; Coleman, J.N. Improved Adhesive Strength and Toughness of Polyvinyl Acetate Glue on Addition of Small Quantities of Graphene. *ACS Appl. Mater. Interfaces* **2013**, *5*, 1423–1428. [CrossRef] [PubMed]
5. Kolya, H.; Kang, C.-W. Polyvinyl acetate/reduced graphene oxide-poly (diallyl dimethylammonium chloride) composite coated wood surface reveals improved hydrophobicity. *Prog. Org. Coat.* **2021**, *156*, 106253. [CrossRef]
6. López-Suevos, F.; Eyholzer, C.; Bordeanu, N.; Richter, K. DMA analysis and wood bonding of PVAc latex reinforced with cellulose nanofibrils. *Cellulose* **2010**, *17*, 398. [CrossRef]
7. Shen, J.; Liang, J.; Lin, X.; Lin, H.; Yu, J.; Wang, S. The Flame-Retardant Mechanisms and Preparation of Polymer Composites and Their Potential Application in Construction Engineering. *Polymers* **2022**, *14*, 82. [CrossRef]

8. Vahidi, G.; Bajwa, D.S.; Shojaeiarani, J.; Stark, N.; Darabi, A. Advancements in traditional and nanosized flame retardants for polymers—A review. *J. Appl. Polym. Sci.* **2021**, *138*, 50050. [CrossRef]
9. Villamil Watson, D.A.; Schiraldi, D.A. Biomolecules as Flame Retardant Additives for Polymers: A Review. *Polymers* **2020**, *12*, 849. [CrossRef] [PubMed]
10. Technical University in Zvolen. Earth in a trap? 2018—Analytical Methods in Fire and Environmental Sciences. In Proceedings of the International Scientific Conference, Salamandra Hotel, Horný Hodrušský tajch, Hodruša-Hámre, Slovak Republic, 2018; Available online: https://kpo.tuzvo.sk/sites/default/files/earth_in_a_trap_2018.pdf (accessed on 10 December 2024).
11. Popescu, C.-M.; Pfriem, A. Treatments and modification to improve the reaction to fire of wood and wood based products—An overview. *Fire Mater.* **2020**, *44*, 100–111. [CrossRef]
12. Choudhury, A.K.R. Advances in halogen-free flame retardants. *Tre. Text. Fash. Desig.* **2018**, *1*, 70–74. [CrossRef]
13. Zybina, O.; Gravit, M. Intumescent Coatings for Fire Protection of Building Structures and Materials. In *Springer Series on Polymer and Composite Materials*; Springer: Berlin/Heidelberg, Germany, 2020.
14. Costes, L.; Laoutid, F.; Brohez, S.; Dubois, P. Bio-based flame retardants: When nature meets fire protection. *Mater. Sci. Eng. R Rep.* **2017**, *117*, 1–25. [CrossRef]
15. Santoni, I.; Pizzo, B. Evaluation of alternative vegetable proteins as wood adhesives. *Ind. Crops Prod.* **2013**, *45*, 148–154. [CrossRef]
16. Zheng, P.; Zeng, Q.; Lin, Q.; Fan, M.; Zhou, J.; Rao, J.; Chen, N. Investigation of an ambient temperature-curable soy-based adhesive for wood composites. *Int. J. Adhes. Adhes.* **2019**, *95*, 102429. [CrossRef]
17. Bai, M.; Huang, Y.; Huang, S.; Wang, S.; Chen, W.; Hou, X.; Gao, Z. A novel wood adhesive based on yeast hydrolysate. *BioResources* **2019**, *14*, 6015–6024. [CrossRef]
18. Kadimaliev, D.; Telyatnik, V.; Revin, V.; Parshin, A.; Allahverdi, S.; Gunduz, G.; Kezina, E.; Asik, N. Optimization of the conditions required for chemical and biological modification of the yeast waste from beer manufacturing to reduce adhesive compositions. *BioResources* **2012**, *7*, 1984–1993. [CrossRef]
19. Kadimaliev, D.; Kezina, E.; Telyatnik, V.; Revin, V.; Parchaykina, O.; Syusin, I. Residual Brewer's Yeast Biomass and Bacterial Cellulose as an Alternative to Toxic Phenol-Formaldehyde Binders in Production of Pressed Materials from Waste Wood. *BioResources* **2015**, *10*, 1644–1656. [CrossRef]
20. Núñez Decap, M.; Ballerini Arroyo, A.; Alarcón Énos, J. Evaluation of single cell protein from yeast for the development of wood adhesives. *Eur. J. Wood Wood Prod.* **2016**, *74*, 821–828. [CrossRef]
21. Núñez-Decap, M.; Ballerini-Arroyo, A.; Alarcón-Enos, J. Sustainable particleboards with low formaldehyde emissions based on yeast protein extract adhesives Rhodotorula rubra. *Eur. J. Wood Wood Prod.* **2018**, *76*, 1279–1286. [CrossRef]
22. Núñez-Decap, M.; Ballerini-Arroyo, A.; Alarcón-Enos, J. Wood-adhesives of Rhodotorula rubra reinforced with glyoxal and resorcinol. *Int. Wood Prod. J.* **2019**, *10*, 111–117. [CrossRef]
23. Lagel, M.C.; Pizzi, A.; Redl, A.; Al-Marzouki, F.M. Phenol-wheat protein-formaldehyde thermoset wood adhesives. *Eur. J. Wood Wood Prod.* **2015**, *73*, 439–448. [CrossRef]
24. Xi, X.; Pizzi, A.; Gerardin, C.; Liao, J.; Amirou, S.; Abdalla, S. Glutaraldehyde-wheat gluten protein adhesives for wood bonding. *J. Adhes.* **2021**, *97*, 88–100. [CrossRef]
25. Cheng, H.N.; Ford, C.; Dowd, M.K.; He, Z. Soy and cottonseed protein blends as wood adhesives. *Ind. Crops Prod.* **2016**, *85*, 324–330. [CrossRef]
26. Pradyawong, S.; Li, J.; He, Z.; Sun, X.S.; Wang, D.; Cheng, H.N.; Klasson, K.T. Blending cottonseed meal products with different protein contents for cost-effective wood adhesive performances. *Ind. Crops Prod.* **2018**, *126*, 31–37. [CrossRef]
27. Muttil, N.; Ravichandra, G.; Bigger, S.W.; Thorpe, G.R.; Shailaja, D.; Singh, S.K. Comparative Study of Bond Strength of Formaldehyde and Soya based Adhesive in Wood Fibre Plywood. *Procedia Mater. Sci.* **2014**, *6*, 2–9. [CrossRef]
28. Mousavi, S.Y.; Huang, J.; Li, K. A cold-set wood adhesive based on soy protein. *Int. J. Adhes. Adhes.* **2021**, *106*, 102801. [CrossRef]
29. Alongi, J.; Carletto, R.A.; Bosco, F.; Carosio, F.; Di Blasio, A.; Cuttica, F.; Antonucci, V.; Giordano, M.; Malucelli, G. Caseins and hydrophobins as novel green flame retardants for cotton fabrics. *Polym. Degrad. Stab.* **2014**, *99*, 111–117. [CrossRef]
30. Beh, J.H.; Yew, M.C.; Saw, L.H.; Yew, M.K. Fire Resistance and Mechanical Properties of Intumescent Coating Using Novel BioAsh for Steel. *Coatings* **2020**, *10*, 1117. [CrossRef]
31. Petkovska, J.; Mladenovic, N.; Leising, W.; Baidak, A.; Temkov, M.; Mirakovski, D.; Dimova, V.; Jordanov, I. Egg white proteins/lignin-DAP intumescent multilayer nanocoating for flame retardant cotton fabric. *Prog. Org. Coat.* **2024**, *186*, 107983. [CrossRef]
32. Dong, L.; Xue, Y.; Huang, H.; Shen, D.; Gao, W.; Xu, F.; Weng, Y.; Zhang, Y. Facile synthesis of soybean protein-based phosphorus-nitrogen flame retardant for poly(lactic acid). *Polym. Degrad. Stab.* **2023**, *214*, 110412. [CrossRef]
33. Xu, F.; Zhang, G.; Wang, P.; Dai, F. Durable and high-efficiency casein-derived phosphorus-nitrogen-rich flame retardants for cotton fabrics. *Cellulose* **2022**, *29*, 2681–2697. [CrossRef]
34. Chen, J.; Liu, Y.; Zhang, J.; Ren, Y.; Liu, X. Synthesis of Novel Arginine-Based Flame Retardant and Its Application in Lyocell Fabric. *Molecules* **2021**, *26*, 3588. [CrossRef]

35. Vishwakarma, A.; Reddy, V.J.; Kandola, B.K.; Kumar, V.; Dasari, A.; Chattopadhyay, S. Egg White Protein-Hypophosphorous Acid Based Fire Retardant Single Bilayer Coating Assembly for Cotton Fabric. *Cellulose* **2021**, *28*, 10689–10705. [CrossRef]
36. Uddin, M.; Kiviranta, K.; Suvanto, S.; Alvila, L.; Leskinen, J.; Lappalainen, R.; Haapala, A. Casein-magnesium composite as an intumescent fire retardant coating for wood. *Fire Saf. J.* **2020**, *112*, 102943. [CrossRef]
37. Albite-Ortega, J.; Sánchez-Valdes, S.; Ramirez-Vargas, E.; Nuñez-Figueredo, Y.; Ramos deValle, L.F.; Martínez-Colunga, J.G.; Graciano-Verdugo, A.Z.; Sanchez-Martínez, Z.V.; Espinoza-Martínez, A.B.; Rodriguez-Gonzalez, J.A.; et al. Influence of keratin and DNA coating on fire retardant magnesium hydroxide dispersion and flammability characteristics of PE/EVA blends. *Polym. Degrad. Stab.* **2019**, *165*, 1–11. [CrossRef]
38. Carosio, F.; Di Blasio, A.; Alongi, J.; Malucelli, G. Green DNA-based flame retardant coatings assembled through Layer by Layer. *Polymer* **2013**, *54*, 5148–5153. [CrossRef]
39. Tang, H.; Zhou, X.-B.; Liu, X.-L. Effect of Magnesium Hydroxide on the Flame Retardant Properties of Unsaturated Polyester Resin. *Procedia Eng.* **2013**, *52*, 336–341. [CrossRef]
40. Jiao, L.-L.; Zhao, P.-C.; Liu, Z.-Q.; Wu, Q.-S.; Yan, D.-Q.; Li, Y.-L.; Chen, Y.-N.; Li, J.-S. Preparation of Magnesium Hydroxide Flame Retardant from Hydromagnesite and Enhance the Flame Retardant Performance of EVA. *Polymers* **2022**, *14*, 1567. [CrossRef]
41. Wang, C.; Wang, Y.; Han, Z. Enhanced flame retardancy of polyethylene/magnesium hydroxide with polycarbosilane. *Sci. Rep.* **2018**, *8*, 14494. [CrossRef]
42. Harwick Standard Distribution Corporation. Magnesium Hydroxide Data Sheet. 2008. ISO 9001-2000 Registered. 60 s. Seiberling St. P.O. Box 9360, Akron, OH 44305-0360. Available online: https://harwick.com/files/tds/MAGNESIUM_HYDROXIDE.PDF (accessed on 5 February 2025).
43. *ASTM D1084-16R21*; Standard Test Methods for Viscosity of Adhesives. ASTM International: West Conshohocken, PA, USA, 2021.
44. *ASTM E70-24*; Standard Test Method for pH of Aqueous Solutions with the Glass Electrode. ASTM International: West Conshohocken, PA, USA, 2024.
45. *ASTM1875-03*; Standard Test Method for Density of Adhesives in Fluid Form. ASTM International: West Conshohocken, PA, USA, 2018.
46. *ASTM D1490-01R18*; Standard Test Method for Nonvolatile Content of Urea-Formaldehyde Resin Solutions. ASTM International: West Conshohocken, PA, USA, 2018.
47. *ASTM D2339-98*; Standard Test Method for Strength Properties of Adhesives in Two-Ply Wood Construction in Shear by Tension Loading. ASTM International: West Conshohocken, PA, USA, 2011.
48. *UNE-EN 314*; Plywood. Bonding Quality. UNE Normalización española: Madrid, España, 2007.
49. *ASTM D1360-98*; Standard Test Method for Fire Retardancy of Paints (Cabinet Method). ASTM International: West Conshohocken, PA, USA, 2017.
50. Garay, R.; Henriquez, M. Comportamiento frente al fuego de tableros y madera de pino radiata con y sin pintura retardante de llama. *Maderas. Cienc. Tecnol.* **2010**, *12*, 11–24. [CrossRef]
51. *ASTM D3418*; Standard Test Method for Transition Temperatures and Enthalpies of Fusion and Crystallization of Polymers by Differential Scanning Calorimetry. ASTM International: West Conshohocken, PA, USA, 2021.
52. *ASTM D5751-99R19*; Standard Specification for Adhesives Used for Laminate Joints in Nonstructural Lumber Products. ASTM International: West Conshohocken, PA, USA, 2019.
53. *ISO 12580*; Timber Structures—Glued Laminated Timber—Methods of Test for Glue-Line Delaminatn. ISO: Geneva, Switzerland, 2007.
54. Miturska, I.; Rudawska, A. Influence of Adhesive Compound Viscosity on the Strength Properties of 1.0503 Steel Sheets Adhesive Joints. *Adv. Sci. Technol. Res. J.* **2022**, *16*, 196–205. [CrossRef]
55. Gavrilovic-Grmusa, I.; Dunky, M.; Miljkovic, J.; Djiporovic-Momcilovic, M. Influence of the viscosity of UF resins on the radial and tangential penetration into poplar wood and on the shear strength of adhesive joints. *Holzforschung* **2012**, *66*, 849–856. [CrossRef]
56. Sedano-Mendoza, M.; Ávila-Calderón, L.E.A.; Jardón-Madrigal, G. Análisis técnico de tres adhesivos comerciales para la industria de muebles. *Ing. Investig. Tecnol.* **2021**, *22*, 1–7. [CrossRef]
57. Ruwoldt, J. A Critical Review of the Physicochemical Properties of Lignosulfonates: Chemical Structure and Behavior in Aqueous Solution, at Surfaces and Interfaces. *Surfaces* **2020**, *3*, 622–648. [CrossRef]
58. Komisarz, K.; Majka, T.M.; Pielichowski, K. Chemical Transformation of Lignosulfonates to Lignosulfonamides with Improved Thermal Characteristics. *Fibers* **2022**, *10*, 20. [CrossRef]
59. Lu, Y.; Wu, C.; Xu, S.-A. Mechanical, thermal and flame retardant properties of magnesium hydroxide filled poly(vinyl chloride) composites: The effect of filler shape. *Compos. Part A Appl. Sci. Manuf.* **2018**, *113*, 1–11. [CrossRef]
60. Liu, H.; Wang, R.; Xu, X. Thermal stability and flame retardancy of PET/magnesium salt composites. *Polym. Degrad. Stab.* **2010**, *95*, 1466–1470. [CrossRef]
61. Saba, N.; Alothman, O.Y.; Almutairi, Z.; Jawaid, M. Magnesium hydroxide reinforced kenaf fibers/epoxy hybrid composites: Mechanical and thermomechanical properties. *Constr. Build. Mater.* **2019**, *201*, 138–148. [CrossRef]

62. Dasaesamoh, A.; Adair, A.; Matchawet, S. Effect of Magnesium Hydroxide on Flame Retardant Properties for Adhesive Materials by Solution Mixing Process. *J. Phys. Conf. Ser.* **2021**, *2049*, 012006. [CrossRef]
63. Neeraj, M.; Aurélie, C.; François, R.; Stéphane, G.; Fabine, S.; Giulio, M.; Guan, J.-P. An Overview on the Use of Lignin and Its Derivatives in Fire Retardant Polymer Systems. In *Lignin*; Matheus, P., Ed.; IntechOpen: Rijeka, Croatia, 2018; Chapter 9.
64. Manals-Cutiño, E.; Penedo-Medina, M.; Giralt-Ortega, G. Análisis termogravimetrico y térmico diferencial de diferentes biomasas vegetales. *Tecnol. Química* **2011**, *31*, 36–43.
65. Manara, P.; Vamvuka, D.; Sfakiotakis, S.; Vanderghem, C.; Richel, A.; Zabaniotou, A. Mediterranean agri-food processing wastes pyrolysis after pre-treatment and recovery of precursor materials: A TGA-based kinetic modeling study. *Food Res. Int.* **2015**, *73*, 44–51. [CrossRef]
66. Tang, H.; Chen, K.; Li, X.; Ao, M.; Guo, X.; Xue, D. Environment-friendly, flame retardant thermoplastic elastomer–magnesium hydroxide composites. *Funct. Mater. Lett.* **2017**, *10*, 1750042. [CrossRef]
67. Fitzsimons, S.M.; Mulvihill, D.M.; Morris, E.R. Denaturation and aggregation processes in thermal gelation of whey proteins resolved by differential scanning calorimetry. *Food Hydrocoll.* **2007**, *21*, 638–644. [CrossRef]
68. Ichimura, M. Impurity Doping in $Mg(OH)_2$ for n-Type and p-Type Conductivity Control. *Materials* **2020**, *13*, 2972. [CrossRef] [PubMed]
69. Al-Mosawi, A. Effect of magnesium oxide additions on electrical conductivity of polyester resin. *Int. J. Adv. Res.* **2013**, *1*, 265–268.
70. Vashisth, A.; Auvil, T.J.; Sophiea, D.; Mastroianni, S.E.; Green, M.J. Using Radio-Frequency Fields for Local Heating and Curing of Adhesive for Bonding Metals. *Adv. Eng. Mater.* **2021**, *23*, 2100210. [CrossRef]
71. Gruener, J.T.; Vashisth, A.; Pospisil, M.J.; Camacho, A.C.; Oh, J.-H.; Sophiea, D.; Mastroianni, S.E.; Auvil, T.J.; Green, M.J. Local heating and curing of carbon nanocomposite adhesives using radio frequencies. *J. Manuf. Process.* **2020**, *58*, 436–442. [CrossRef]
72. Qiao, L.; Easteal, A.J.; Bolt, C.J.; Coveny, P.K.; Franich, R.A. The effects of filler materials on poly(vinyl acetate) emulsion wood adhesives. *Pigment Resin Technol.* **1999**, *28*, 326–330. [CrossRef]
73. Cailloux, J.; Abt, T.; Garcia-Masabet, V.; Santana Perez, O.; Sanchez-Soto, M.; Carrasco, F.; Maspoch, M. Effect of the viscosity ratio on the PLA/PA10.10 bioblends morphology and mechanical properties. *Express Polym. Lett.* **2018**, *12*, 569–582. [CrossRef]
74. Kaboorani, A.; Riedl, B. Improving performance of polyvinyl acetate (PVA) as a binder for wood by combination with melamine based adhesives. *Int. J. Adhes. Adhes.* **2011**, *31*, 605–611. [CrossRef]
75. Ye, R.; Wang, C.; Shi, X.; Zhang, D.; Lai, C.; Chen, X.; Wang, C.; Chu, F. A facile strategy to fabricate low viscosity and high cold tack soy protein-based adhesive for particleboard production. *Ind. Crops Prod.* **2024**, *214*, 118612. [CrossRef]
76. Zeng, N.; Xie, J.J.; Ding, C. Properties of the Soy Protein Isolate/PVAc Latex Blend Adhesives. *Adv. Mater. Res.* **2012**, *550–553*, 1103–1107. [CrossRef]
77. Zhang, K.; Hu, H.; Li, S.; He, Y.; Guo, J. Effect of sodium dodecyl sulfate (SDS) on mechanical performance of polyvinyl-acetate-based emulsion polymer isocyanate. *Int. J. Adhes. Adhes.* **2020**, *98*, 102539. [CrossRef]
78. Klapiszewski, Ł.; Tomaszewska, J.; Skórczewska, K.; Jesionowski, T. Preparation and Characterization of Eco-Friendly $Mg(OH)_2$/Lignin Hybrid Material and Its Use as a Functional Filler for Poly(Vinyl Chloride). *Polymers* **2017**, *9*, 258. [CrossRef]
79. Gomes Ferreira, J.; Cruz, H.; Silva, R. Failure behaviour and repair of delaminated glulam beams. *Constr. Build. Mater.* **2017**, *154*, 384–398. [CrossRef]
80. Fodor, F.; Bak, M. Studying the Wettability and Bonding Properties of Acetylated Hornbeam Wood Using PVAc and PUR Adhesives. *Materials* **2023**, *16*, 2046. [CrossRef]
81. Hass, P.; Wittel, F.K.; Mendoza, M.; Herrmann, H.J.; Niemz, P. Adhesive penetration in beech wood: Experiments. *Wood Sci. Technol.* **2012**, *46*, 243–256. [CrossRef]
82. Kamke, F.A.; Lee, J.N. Adhesive Penetration in Wood—A Review. *Wood Fiber Sci.* **2007**, *39*, 205–220.
83. de Oliveira, R.G.E.; Gonçalves, F.G.; Segundinho, P.G.d.A.; Oliveira, J.T.d.S.; Paes, J.B.; Chaves, I.L.S.; Brito, A.S. Analysis of glue line and correlations between density and anatomical characteristics of Eucalyptus grandis × Eucalyptus urophylla glulam. *Maderas. Cienc. Tecnol.* **2020**, *22*, 495–504. [CrossRef]
84. Laoutid, F.; Duriez, V.; Brison, L.; Aouadi, S.; Vahabi, H.; Dubois, P. Synergistic flame-retardant effect between lignin and magnesium hydroxide in poly(ethylene-co-vinyl acetate). *Flame Retard. Therm. Stab. Mater.* **2019**, *2*, 9–18. [CrossRef]
85. Pettersen, R.C. The Chemical Composition of Wood. In *The Chemistry of Solid Wood*; Advances in Chemistry; American Chemical Society: Washington, DC, USA, 1984; Volume 207, pp. 57–126.
86. Madyaratri, E.W.; Ridho, M.R.; Aristri, M.A.; Lubis, M.A.; Iswanto, A.H.; Nawawi, D.S.; Antov, P.; Kristak, L.; Majlingová, A.; Fatriasari, W. Recent Advances in the Development of Fire-Resistant Biocomposites—A Review. *Polymers* **2022**, *14*, 362. [CrossRef]
87. Yauk, M.; Stenson, J.; Donor, M.; Van Den Wymelenberg, K. Evaluating Volatile Organic Compound Emissions from Cross-Laminated Timber Bonded with a Soy-Based Adhesive. *Buildings* **2020**, *10*, 191. [CrossRef]
88. Henríquez, F.; Hernández, D.; Varas-Concha, F.; Gutierrez, C.; Quinteros-Lama, H.; Morales-Ferreiro, J.O. VOCs and PM listing of Eucalyptus globulus combustion in residential wood stoves. *Maderas. Cienc. Y Tecnol.* **2023**, *25*, 12. [CrossRef]

89. D'Andrea, M.A.; Reddy, G.K. Health Risks Associated With Benzene Exposure in Children: A Systematic Review. *Glob. Pediatr. Health* **2018**, *5*, 2333794X18789275. [CrossRef]
90. Desservettaz, M.; Pikridas, M.; Stavroulas, I.; Bougiatioti, A.; Liakakou, E.; Hatzianastassiou, N.; Sciare, J.; Mihalopoulos, N.; Bourtsoukidis, E. Emission of volatile organic compounds from residential biomass burning and their rapid chemical transformations. *Sci. Total Environ.* **2023**, *903*, 166592. [CrossRef] [PubMed]
91. McKennon, M.J.; Meyers, A.I.; Drauz, K.; Schwarm, M. A convenient reduction of amino acids and their derivatives. *J. Org. Chem.* **1993**, *58*, 3568–3571. [CrossRef]
92. Kondo, S.-I.; Abe, S.; Katagiri, H. Synthesis and photophysical properties of cyclosiloxanes with substituted naphthyl groups. *Dye. Pigment.* **2023**, *217*, 111394. [CrossRef]
93. López Pérez, J.P.; Boronat Gil, R. Estudio de la inhibición de la respiración/fermentación en células de levadura por fluoruro de sodio. *Study Inhib. Respir./Ferment. Yeast Cells Sodium Fluoride* **2013**, *10*, 133–138. [CrossRef]
94. Maicas, S. The Role of Yeasts in Fermentation Processes. *Microorganisms* **2020**, *8*, 1142. [CrossRef]
95. Li, Y.; Lu, J.; Yin, X.; Liu, Z.; Tong, Y.; Zhou, L. Indoor phthalate concentrations in residences in Shihezi, China: Implications for preschool children's exposure and risk assessment. *Environ. Sci. Pollut. Res.* **2019**, *26*, 19785–19794. [CrossRef]
96. Paris, E.; Carnevale, M.; Vincenti, B.; Palma, A.; Guerriero, E.; Borello, D.; Gallucci, F. Evaluation of VOCs Emitted from Biomass Combustion in a Small CHP Plant: Difference between Dry and Wet Poplar Woodchips. *Molecules* **2022**, *27*, 955. [CrossRef]
97. Herbinet, O.; Bax, S.; Fau-Glaude, P.-A.; Glaude Pa Fau-Carré, V.; Carré, V.; Fau-Battin-Leclerc, F.; Battin-Leclerc, F. Mass spectra of cyclic ethers formed in the low-temperature oxidation of a series of n-alkanes. *Fuel* **2011**, *90*, 528–535. [CrossRef]
98. Bhushan, R.; Lal, M. Enantioseparation of amino alcohols by reversed-phase high-performance liquid chromatography using cyanuric chloride-based chiral derivatizing reagents having amino acids and their amides as chiral auxiliaries. *Acta Chromatogr.* **2014**, *26*, 413–427. [CrossRef]
99. Estrada Leon, A.; Ramamurthy, R.; Ghysels, S.; Niazi, S.; Prins, W.; Ronsse, F. Analytical (hydro)pyrolysis of pinewood and wheat straw in chloride molten salts: A route for 2-methyl furan production. *Fuel Process. Technol.* **2023**, *250*, 107917. [CrossRef]
100. Herreño Gallego, S.A. Evaluación de la polimerización de vinil acetato en emulsión núcleo-coraza con una emulsión polivinílica como semilla. *Rev. Investig.* **2020**, *13*, 45–55. [CrossRef]
101. Yang, X.; Huang, J.; Yang, Y.; Ye, C.; Wang, Y.; Liu, Y.; Wang, F.; Sun, N.; Yu, W. Effect of ammonium acetate on alcohol fermentation in cassava-alcohol fermentation process. *Microbiol. Res.* **2022**, *256*, 126868. [CrossRef] [PubMed]
102. Lin, C.-F.; Karlsson, O.; Mantanis, G.; Jones, D.; Sandberg, D. Morphology Influence of Fire-Retardant Additives on Melamine Formaldehyde Resin Modified Wood. In Proceedings of the 16th Annual Meeting of the Northern European Network for Wood Science and Engineering (WSE2020), Helsinki, Finland, 1–2 December 2020.
103. Camargo, A.; Ibáñez, C.M. Fire performance of Pinus taeda wood treated with zinc borate before and after leaching. *Maderas. Cienc. Tecnol.* **2024**, *26*, 1–14. [CrossRef]
104. Ma, G.; Wang, X.; Cai, W.; Ma, C.; Wang, X.; Zhu, Y.; Kan, Y.; Xing, W.; Hu, Y. Preparation and Study on Nitrogen- and Phosphorus-Containing Fire Resistant Coatings for Wood by UV-Cured Methods. *Front. Mater.* **2022**, *9*, 851754. [CrossRef]
105. Yan, L.; Xu, Z.; Liu, D. Synthesis and application of novel magnesium phosphate ester flame retardants for transparent intumescent fire-retardant coatings applied on wood substrates. *Prog. Org. Coat.* **2019**, *129*, 327–337. [CrossRef]
106. Balzano, A.; Merela, M.; Čufar, K. Scanning Electron Microscopy Protocol for Studying Anatomy of Highly Degraded Waterlogged Archaeological Wood. *Forests* **2022**, *13*, 161. [CrossRef]
107. Sturm, H.; Schartel, B.; Weiß, A.; Braun, U. SEM/EDX: Advanced investigation of structured fire residues and residue formation. *Polym. Test.* **2012**, *31*, 606–619. [CrossRef]
108. Gadhave, R.V.I.; Dhawale, P.V. State of Research and Trends in the Development of Polyvinyl Acetate-Based Wood Adhesive. *Open J. Polym. Chem.* **2022**, *12*, 13–42. [CrossRef]
109. Salvini, A.; Saija, L.; Finocchiaro, S.; Gianni, G.; Giannelli, C.; Tondi, G. A New Methodology in the Study of PVAc-Based Adhesive Formulations. *J. Appl. Polym. Sci.* **2009**, *114*, 3841–3854. [CrossRef]